Voyager Interstellar Mission

Proposal to Senior Review 2010 of the Mission Operations and Data Analysis Program for the Heliophysics Operating Missions

Edward C. Stone, Project Scientist
John D. Richardson, Proposal Editor
Ed B. Massey, Project Manager

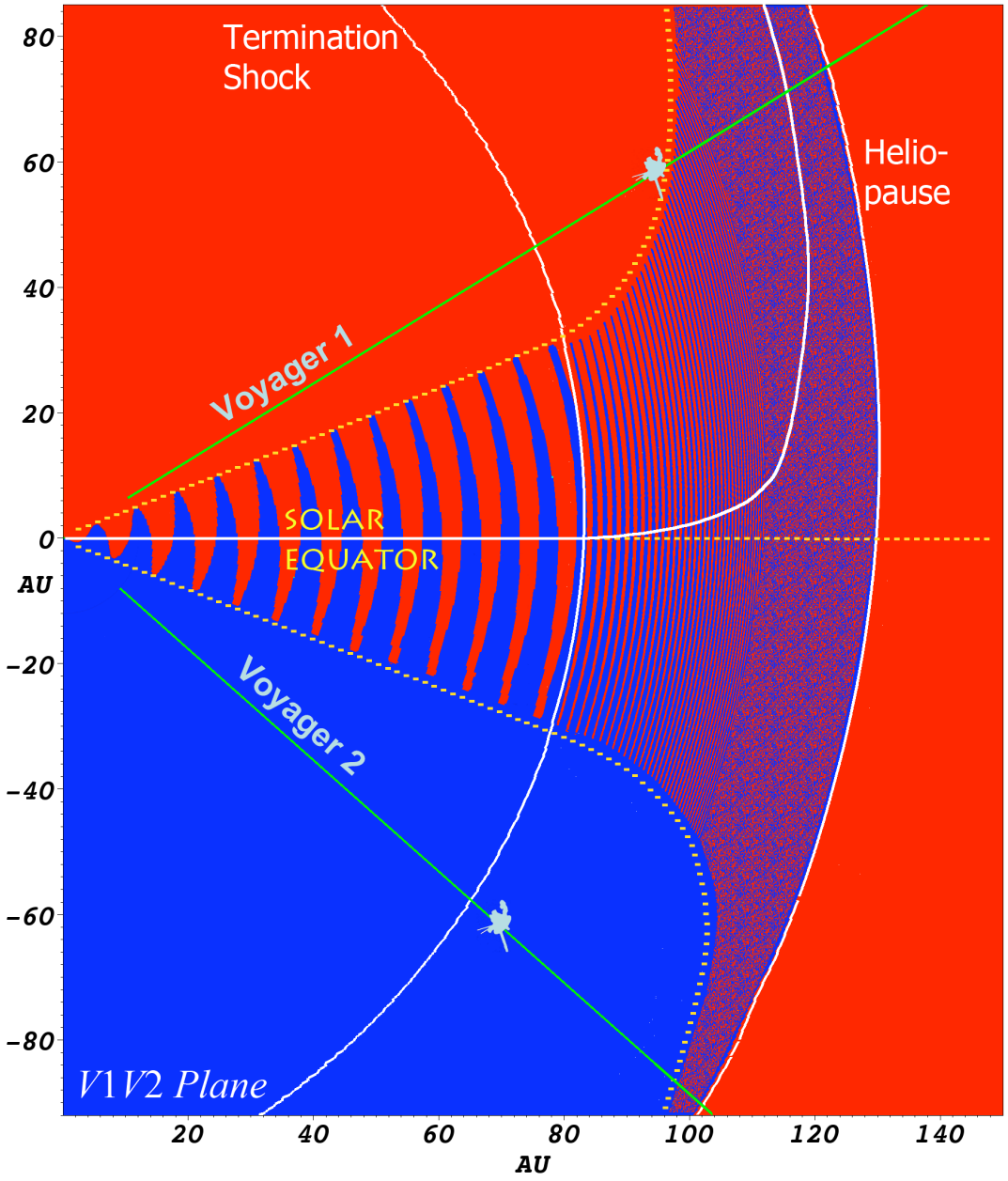

March 2010

EXECUTIVE SUMMARY

The Voyager Interstellar Mission is exploring the interaction of the heliosphere with the local interstellar medium (LISM). Voyager 1 (V1) and Voyager 2 (V2) are both in the heliosheath, making the first in situ observations of the shocked solar wind beyond the termination shock (TS). The heliosheath extends to the heliopause; beyond the heliopause is the interstellar medium. The goal of the Voyager Interstellar Mission, as the name implies, is to make the first in situ observations of the region outside our heliosphere.

As the Voyagers proceed outward toward that goal, they are making measurements of totally unexplored regions of the heliosphere. The Voyager crossings of the TS provided the first concrete information on the scale size and the shape of the heliosphere. Voyager 1, in the northern hemisphere of the heliosphere, crossed the TS at 94 Astronomical Units (AU) while V2, in the southern hemisphere, crossed it at 84 AU. Based on these TS distances and model predictions, the heliopause (HP) and LISM are probably 30-50 AU further out. The asymmetry in the TS crossing distances verifies that the southern hemisphere of the heliosphere is pushed inward, probably by the interstellar magnetic field. Although the uncertainties in the HP position are large, the Voyager spacecraft have a good chance of reaching this boundary in their operational lifetimes. The observed asymmetry may allow V1 and V2 to cross the HP at roughly the same time and provide simultaneous observations of the LISM.

The V1 and V2 TS and heliosheath observations provided many surprises that we are still working to understand. A major outstanding problem is the source of the anomalous cosmic rays (ACRs). Before the Voyager TS crossings, the ACRs were thought to be accelerated at the TS. The ACR source was not found at either Voyager TS crossing; new hypotheses place the source either in the flanks of the TS or nearer to the heliopause. Plasma flows in the heliosheath are also a puzzle, with radial flows at V2 a factor of two greater than at V1 and flows at V2 more tangential than meridional, both contrary to predictions. The heliosheath magnetic field is highly variable on time scales of tens of minutes to hours, showing that this region is very dynamic. None of the foregoing observations were anticipated. These and future revelations of the unexpected nature of the heliosheath, HP, and LISM will continue to drive theoretical modeling leading to improved understanding of the physics of the heliosheath.

The current solar minimum has been very long and very deep. The solar wind plasma dynamic pressure and magnetic field strength are at record lows. The tilt of the heliospheric current sheet only recently reached the low levels of previous solar minimum. Over the next few years these solar conditions will reach the Voyager spacecraft and the heliospheric boundaries. The Voyagers are already entering the interaction region between the fast and slow solar wind and are near the maximum extent of the heliospheric current sheet (HCS), which separates regions of inward and outward magnetic polarity. As the HCS tilt decreases the Voyagers should be at high enough latitudes to monitor the interaction region between the fast and slow solar wind and to observe coronal hole flow in the heliosheath. As the solar cycle proceeds and solar activity increases, we will learn how interplanetary coronal mass ejections (ICMEs) and merged interaction regions (MIRs) propagate through and affect the heliosheath. We will observe the recovery of cosmic rays beyond 100 AU at solar minimum and observe the start of the next modulation cycle, determine the effects of a negative magnetic polarity solar cycle on the cosmic rays, and monitor the unfolding of the low-energy ACR spectra at V1 and V2.

An exciting new scientific opportunity is presented by the Interstellar Boundary Explorer (IBEX) mission. This spacecraft observes neutral atoms generated by charge exchange in the inner and outer heliosheaths and its goal is to understand the global properties of the heliosphere, making all-sky maps of the energetic neutral atoms every six months. Voyager in situ observations of the plasma and particle distributions are critical for the understanding the source of the neutrals observed by IBEX and IBEX gives us a chance to put the Voyager observations into a global perspective.

1. INTRODUCTION

The Voyager spacecraft were launched in 1977 on a trajectory toward the giant planets, which serendipitously was also toward the nose of the heliosphere. After the successful planetary encounters, the Voyager Interstellar Mission continued outward with the goal of making the first observations of the LISM. Both Voyagers have crossed the TS, so the goal of reaching the LISM seems achievable.

The cover figure shows a model of the heliosphere with the Voyager trajectories superposed (courtesy of S. Borovikov and N. Pogorelov). The color scale shows the magnetic field sector. The model is run for solar minimum conditions with the HCS tilted 20° from the solar equator. The HCS varies sinusoidally in the supersonic solar wind upstream of the termination shock. At 80-100 AU, the solar wind encounters the TS and becomes subsonic. The flow speed in the heliosheath beyond the TS is much smaller than in the solar wind, so the HCS is compressed. The outward speed further slows as the plasma approaches the HP, the boundary

between the solar wind and interstellar medium. The HCS becomes too compact for the model to resolve; these compressed current sheets may reconnect and accelerate particles near the HP (Lazarian and Opher, 2009; Drake et al., 2010).

The flow in the heliosheath diverts to carry plasma down the heliotail; the flow in this model has a large poleward component in the northern hemisphere which carries the HCS northward toward the V1 location. V2 is not close to the HCS in this model. The TS and HP are asymmetric, closer to the Sun in the south (V2 direction) than the north (V1 direction) due to the direction of the LISM magnetic field. The HP is expected to be several tens of AU beyond the TS. Beyond this boundary may be a bow shock where the incoming LISM plasma would undergo a shock transition if it were supersonic. The region between the HP and bow shock is known as the outer heliosheath.

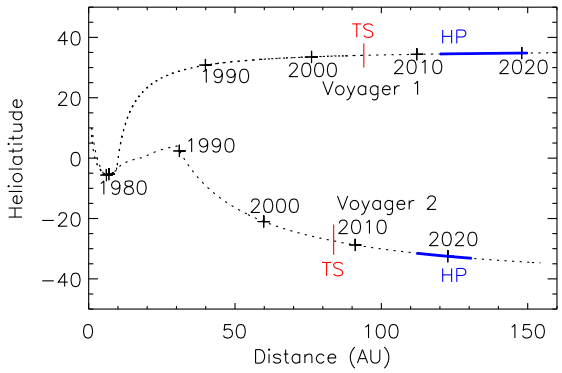

FIGURE 1. Trajectories of the Voyager spacecraft.

The V1 crossing of the TS set the scale for the whole heliospheric system. The missing piece before this crossing was the pressure in the LISM. Knowing the TS boundary distance fixes this parameter. Models predict that the HP is 30-50% more distant than the TS. The V2 crossing of the TS revealed that the heliosphere was asymmetric; the boundaries in the south are closer to the Sun than those in the north. The Voyager trajectories are shown in Figure 1. Distance in AU is plotted vs. heliolatitude and times are marked on the trajectory traces. Also marked are the locations of the V1 and V2 TS crossings and the V1 and V2 HP crossings based on model results. Both the V1 and V2 HP crossings are likely to occur between 2015 and 2020. The spacecraft have sufficient power to operate all instruments until at least 2016; after this time, power-sharing can extend the useful life of the spacecraft beyond 2023. Thus the Voyagers are likely to provide the first in situ measurements of the LISM.

On their way to the LISM, the Voyager spacecraft are exploring an entirely new region, the heliosheath. The data show that this region of subsonic flow is very active, with large fluctuations in the plasma and magnetic field over times scales of hours to days. These variations likely result both from structures entrained in the solar wind and from those generated by the motions of the TS and possibly also the HP. Large fluctuations in MeV particle fluxes are observed but not yet understood. This region contributes to the modulation of the galactic cosmic rays (GCRs) [McDonald et al., 2002]. Unanticipated attributes are being discovered, such as much lower than predicted plasma temperatures, very different plasma speeds at V1 and V2, and an increase of ACR intensities with distance.

The Voyager spacecraft are relatively healthy. The active instrument teams are the Plasma Science experiment (PLS) which measures thermal plasma, the Low Energy Charged Particle experiment (LECP) which detects particles in the tens of keV to tens of MeV range, the Cosmic Ray subsystem (CRS) which measures GCRs and ACRs, the magnetometer experiment (MAG), and the Plasma Wave subsystem (PWS) which observes plasma and radio waves. The V1 PLS experiment failed soon after the Saturn encounter in 1980 and has not been able to detect even the higher plasma fluxes in the heliosheath, but the V2 PLS experiment is returning excellent data from the heliosheath. The V2 PWS returns valuable data in many channels and detected emissions at the TS crossing; however, the wideband receiver failed in 2003, the 17.8 Hz channel is intermittent, and the upper 8 channels (1 kHz to 56 kHz) have decreased sensitivity due to a failure in a multiplexor switch in the FDS. The V2 MAG experiment has a continuing problem with noise generated by the spacecraft and other instruments which makes reliable analysis very difficult, but the higher magnetic field strengths in the heliosheath have made that problem more tractable. Otherwise the instruments work well and all have the sensitivity to continue observations in the environments expected in the heliosheath and in the LISM.

The NASA Heliophysics Roadmap 2009-2030 lists open scientific questions which need to be addressed by current missions. Voyager provides a unique platform for studying many of these questions. The Roadmap also lists three broad scientific and exploration objectives. The first is to understand basic physical processes of the space environment as they occur from the Sun to the interstellar medium, with research focus areas of 1) magnetic reconnection, 2) particle acceleration and transport, 3) ion-neutral interactions, and 4) magnetic dynamos and how they drive the solar environment. The second two broad topics are to understand Earth and its interaction with the heliosphere and to understand the full heliospheric environment.

Magnetic reconnection may be important in several contexts in the outer heliosphere. The solar wind mag-

netic field may reconnect with the interstellar magnetic field, which would accelerate particles and has been suggested as a source of the heliospheric radio emissions [Swisdak et al., 2010]. Reconnection could also occur within the heliosheath itself; the slowdown of the flow near the HP compresses the HCS which could drive reconnection and possibly accelerate the ACRs [Lazarian and Opher, 2009; Drake et al., 2010]. The Voyager spacecraft will enter these hypothesized reconnection regions and observe whether reconnection is important in the outer heliosphere.

The focus area of particle acceleration and transport is also uniquely addressed by the Voyager spacecraft. The pre-Voyager paradigm that ACRs were pickup ions accelerated at the TS was challenged by the observation that the ACR source was not observed at the V1 or V2 TS crossings. The Voyagers did discover an energetic particle population with energies from tens of keV to a few MeV which is accelerated at the TS, but we still do not know the source of the ACRs. Further Voyager observations should provide an answer to this question.

Ion-neutral interactions are a key to understanding Voyager observations and the interaction of the heliosphere with the interstellar medium. Voyager first revealed the importance of the pickup ions for balancing the pressure in solar wind structures and the significant slowing of the solar wind from pickup of the ISM neutrals. At the TS, most of the solar wind flow energy went into heating these pickup ions. IBEX is now measuring the energetic neutral atoms (ENAs) generated by charge exchange in the heliosheath, giving a global view of the heliosphere. The ion distributions observed by the Voyager spacecraft are crucial for interpreting the IBEX results and the IBEX results allow the Voyager results to be put into a global context.

The Voyager Interstellar mission is also a critical part of many "priority investigations" listed in the Roadmap:

"How are plasmas and charged particles heated and accelerated?"

"How do solar wind disturbances propagate and evolve through the solar system?"

"How do the heliosphere and interstellar medium interact?"

"What is the magnetic structure of the Sun-Heliosphere system?"

The Voyagers are the only spacecraft positioned to directly observe the boundaries of the heliosphere and to directly sample the LISM. These boundaries are the largest structures in the heliosphere and allow us to study physical processes such as magnetic reconnection, particle acceleration and transport, and the interaction of the solar wind plasma with the LISM neutrals in a system with scale size $\sim$100 AU.

The recent scientific discoveries bearing on these Roadmap objectives are elaborated on in this proposal. They include the first observations of the TS, the first characterization of the plasma and magnetic field environment of the heliosheath, verification of asymmetries in the heliospheric shape, and the lack of ACR acceleration at the TS.

The Voyagers are the outermost spacecraft in NASA's Heliophysics System Observatory, the ensemble of spacecraft collecting data to provide a global picture of heliospheric processes. Voyager plays a critical role and benefits greatly from its place in this observatory. Voyager provides direct observation of ACRs near their source region and of GCRs before they are modulated by the supersonic solar wind. Comparison of 1 AU and Ulysses data with Voyager data has provided tests of models of solar wind evolution. We are working to understand how changes in the solar wind propagate through the heliosheath. Inner heliospheric spacecraft provide data on the solar wind pressure, which controls the motion of the TS and HP. These spacecraft also monitor large solar wind structures such as ICMEs which should cause disturbances in the heliosheath. Models can be used to determine how the solar wind observed in the inner heliosphere evolves with distance and thus give us a rough idea of the solar wind conditions upstream of the TS. These data will help us understand and differentiate the effects of shock motion and solar wind changes on the heliosheath.

The Voyagers observe the integrated effects of solar wind evolution and interaction with the LISM from the inner to outer heliosphere. The inner heliospheric spacecraft do the reverse, observing the integrated effects of inward motion of ACRs, GCRs, and LISM neutrals from the LISM and TS to 1 AU. These complementary data sets allow us to test models, providing input conditions at one boundary and benchmark observations at the other.

The addition of the Interstellar Boundary Explorer (IBEX) spacecraft to the heliospheric observatory has made the role of Voyager even more critical. IBEX measures properties of heliospheric boundary regions by observing energetic neutral atoms. These observations have provided a global picture of the Sun-LISM interaction which is complementary to the simultaneous Voyager in situ measurements. Voyager directly measures the ions that are the neutral source population. Knowledge of the ENA source is critical for understanding the IBEX data. The global picture obtained by IBEX will be of great help for understanding the in situ observations and vice versa.

The minimum of solar activity at the end of solar cycle 23 may finally be near. The average magnetic field strength in the solar wind at 1 AU has reached the lowest annual value ever measured, 4 nT. The interval

of weak magnetic fields is broad, from 2007 into 2010. Since the propagation time of the solar wind from one AU to V1 and V2 is a few years, V1 and V2 have observed the heliosheath in its "ground state" (i.e. free of major disturbances related to solar activity) since the beginning of 2008. The maximum latitudinal extent of the HCS has been below the latitude of Voyager 1 and close to the latitude of Voyager 2 since the beginning of 2008, and the HCS tilt is now decreasing. During the 2010 and 2011, both Voyager spacecraft will probably be above the HCS and influenced primarily by the fast solar wind, which we think is relatively simple. The effects of the increasing solar activity in solar cycle 24 may be seen in the heliosheath in 2011 or soon after. For at least a few years after that one expects to observe significant effects of solar activity in the heliosheath.

Although the position of the heliopause is not known, the time for the Voyager spacecraft to move through the heliosheath will almost certainly be of order of the duration of the solar cycle. Thus, we must consider the effects of the solar cycle on the structure and dynamics of the heliosheath. We are fortunate to have the opportunity to first study the heliosheath in the simplest conditions associated with solar minimum and the onset of solar activity before we confront the additional difficulties associated with major solar activity. It is very important that we thoroughly examine the relatively simple conditions in the heliosheath that will be observed during the next few years. An understanding of these conditions will be necessary before we can interpret the more complicated observations associated with the active Sun.

The sections which follow describe five broad science topics being addressed by the Voyager spacecraft. These topics are 1) a global view of Voyager and IBEX observations, 2) the heliosheath, 3) anomalous cosmic rays, 4) the HP and interplanetary medium, and 5) cosmic ray modulation. For each topic we give a description of the science, summarize recent results, and describe how Voyager data will advance our knowledge in these areas in the future.

2. THE GLOBAL HELIOSPHERE AND BEYOND

2.1 Voyager and IBEX

Our understanding of the way in which the interstellar plasma, neutrals and magnetic field control the global structure of the heliosheath is rapidly evolving. The first results and interpretation of data from the IBEX mission and the independent measurements from the INCA imager on Cassini were published in Science on 15 October 2009. Figure 2 shows the ENA ribbon observed by IBEX and the V1 and V2 locations [McComas et al., 2009]. More detailed analysis of the ENA images from IBEX (energy range 0.5-4.5 keV) and from Cassini INCA (energy range 8-44 keV) and correlation of these data with Voyager 1/2 in situ plasma, magnetic field, and energetic particle data were presented two months later at the Fall 2009 meeting of the American Geophysical Union. The heliosheath is a much more complicated object than the initial interpretations suggested. New conjectures and theoretical interpretations have appeared, not all of which agree.

The critical quantities for the dynamic balance that must be maintained in the heliosheath are the ram pressure of the interstellar plasma (moderately well known), the strength and direction of the interstellar magnetic field (not well determined), and the nonthermal pressures in the inner heliosheath. The last-mentioned quantities are essential to our quantitative understanding of the heliosheath and its transition to the surrounding interstellar plasma flow, because we now realize that the heliosheath constitutes a plasma regime unlike any that we have measured during the entire half-century of space physics exploration.

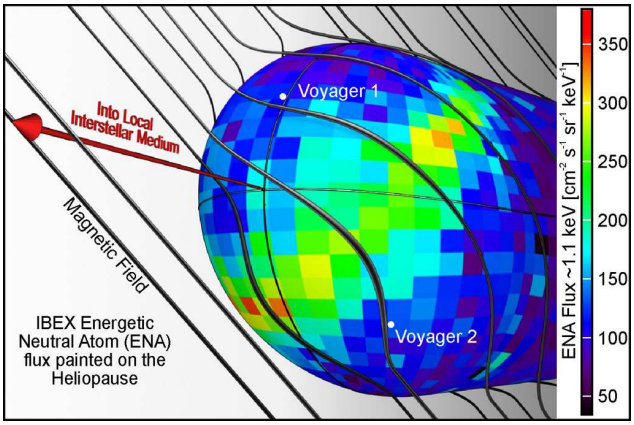

FIGURE 2. Map of ~1.1 keV H emission observed by IBEX. The locations of V1, V2, and the nose of the heliosphere are also shown.

The Voyagers play an invaluable role in establishing "ground truth" at two points within the heliosheath. Dramatic as they are, the IBEX and Cassini/INCA ENA images integrate the superthermal proton intensities (weighted by the neutral H-atom densities) along lines of sight (LOS) many tens of AU in length. Only the Voyager spacecraft can provide guidance as to the distribution of the energetic protons along these ENA lines of sight.

Dramatic temporal changes in prominent ENA features based on the first two IBEX all-sky images, which were taken 6 months apart, will be reported at up-

coming conferences (IBEX/VGR/Cassini Workshop, San Antonio, 9-11 March, 2010; 9th International Astrophysics Conference, Maui, 14-19 March). These changes in the ENA features must be related to temporal changes in the 0.4-6 keV protons in the inner heliosheath or changes in the neutrals formed in the supersonic solar wind because of the long transit times of the ENAs to 1 AU (∼1 year for 1 keV H). These evolving populations are related to the temporal changes observed in the thermal and non-thermal protons measured by Voyager, because all three components (thermal, non-thermal pickup ions, and energetic ions) are required to satisfy the generalized Rankine-Hugoniot conditions for the conservation of mass, momentum, and energy across the termination shock. Furthermore, the Voyager measurements have demonstrated that temporal changes in the total ion pressure can be identified directly and causally with reconfigurations of the global velocity dependence of the solar wind emanating from changing patterns in the polar coronal holes on the Sun.

In summary, the Voyagers are proving to be invaluable and irreplaceable scientific resources in developing our understanding of this most recently discovered and novel plasma regime—the heliosheath and its transition to the interstellar medium.

3. HELIOSHEATH

3.1 Recent Progress: A quick summary

The Voyager 2 TS crossing was featured in a series of papers in Nature, 3 July 2008. Highlights of the results reported in these and subsequent papers are:

1. First observations of the TS

a) The TS is a quasi-perpendicular shock with a shock strength ∼2

b) Most of the plasma flow energy heats the pickup ions, not the thermal plasma

c) The TS has rapid time variations: the three crossings were very different in structure.

d) ACRs were not accelerated at the TS.

e) TSP particles, discovered by V1 and V2 upstream of the TS, are accelerated at the TS.

2. First observations of the heliosheath

a) Flows and fields are highly variable.

b) Radial speed is greater at V2 than V1

c) V2 flows larger in tangential than meridional direction.

d) V2 radial speed constant for first two years in the heliosheath

e) V1 radial speed decreases across the heliosheath.

f) ACR intensities increase with time in the heliosheath

g) Plasma density, temperature, and magnetic field strength have decreased in the heliosheath

The following sections expand on these recent observations and interpretation of the heliosheath data.

3.2 Plasma in the heliosheath

The plasma experiment on Voyager 2 (V2) is providing the first measurements of the thermal plasma in the heliosheath. The instrument measures electrons and ions in the energy/charge range 10-5950 eV. The observed spectra are fit with convected isotropic Maxwellian distributions; the speed, flow angles in the RT and RN planes, proton density and proton temperature in the heliosheath are shown in Figure 3. (We use the standard RTN coordinate system, where R is radially outward, T is parallel to the solar equator and positive in the direction of solar rotation, and N completes a right-handed system.) The average speed was about 150 km/s until 2009.5 and then started to decrease. The density fell by a factor of 2 between the TS crossing and 2008.7 and has remained near 0.001 cm^{-3} through 2009. The density variations are smaller after 2008.7 than near the TS crossing. The temperature also decreased from the TS to 2008.5, then remained constant at about 50,000 K, roughly 1/2 the post-TS value.

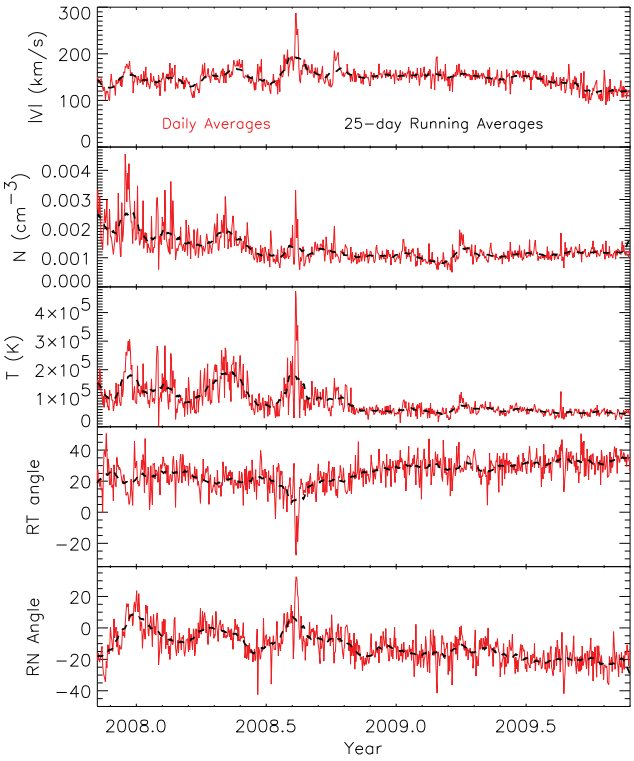

FIGURE 3. Plasma speed, density, temperature, and flow angles observed in the heliosheath by V2. The red lines shows daily averages and the black dashed line 25-day running averages.

Plasma flow velocities in the heliosheath were expected to be directed away from the nose of the heliosphere, with the flows turning away from radial as the Voyager spacecraft moved across the heliosheath. V1 is at northern heliographic latitude 34°N and at a heliographic inertial longitude of 173° which places it almost directly north of the heliospheric nose. V2 is at southern latitude 29°S and longitude 217°, about 44° counterclockwise from V1 and the nose.

Figure 4 shows a schematic diagram of the heliosphere looking from the Sun to the nose of the heliosphere which shows the locations of V1 and V2. V2 is offset from the nose roughly equally in the T and -N directions, so that flow away from the nose would be in the T and -N directions. Before 2008.7, the average flow angles were away from the nose but were highly variable (Figure 3). A 110-day periodicity in V_N was observed, which resulted in +N flow for significant periods. After 2008.7, the flow angles increase with time, consistent with the heliosheath flow turning down the heliotail.

Even though V2 is offset from the nose equally in the V_T and V_N directions, the observed flows are larger in the T than N direction. This flow speed difference originated at the TS and has continued through the heliosheath. Since the initial deflection of the solar wind occurs at the TS, perhaps because the average TS normal is at an angle to the flow, the flow angles may be tracers of the TS shape. These flows (and probably the TS shape) are modified by the interstellar magnetic field [Opher et al., 2009]. As shown by Figure 4, the flows angles observed would result from a TS which is more blunt in the T than N directions, which suggests that the TS is flattened at the poles. This proposed shape differs from model predictions. IBEX should be able to test this hypothesis.

Figure 5 shows the heliosheath plasma flow velocity components V_R, V_T, and V_N measured by the V2 PLS instrument and the V1 LECP instrument; MHD model results are also shown [Pogorelov et al., 2009a]. At V1, V_R and V_T are estimated from a Compton-Getting analysis of LECP low-energy ion angular data taken in a plane nearly parallel to the R-T plane. V_N cannot be determined from the V1 data. The model predicts a decrease in V_R across the heliosheath of -11 km/s/yr; the actual V2 V_R profile is flat until 89 AU with an average speed of 135 km/s. At 89 AU, V_R began to decrease at V2 and is now consistent with the model values. For 0.5 yr (1.8 AU) after the V1 TS crossing, V_R and V_T fluctuated about zero due to the inward radial motion of the TS [Jokipii, 2005]. From 96-102 AU, the V1 observed four large variations in V_R. The average V_R was ∼65 km/s, much lower than both the model predictions and the values measured at V2. The magnitudes of V_T at V1 (41 km/s) and V2 (50 km/s) are roughly equal but in opposite directions, even though V1 is near the T-axis and flow away from the nose would give a small V_T component. The V_N flows at V2 are southward as expected, but smaller in magnitude than the V_T flows, whereas the model predicts similar magnitudes. The non-radial flows at both V1 and V2 differ significantly from the model predictions. Thus even such a basic parameter as the flow field in the heliosheath is not understood and we are continuing our modeling efforts to try to understand the origins of the observed flow speeds.

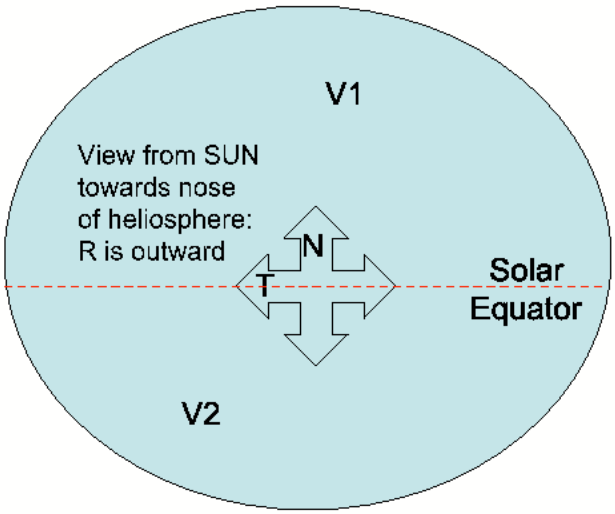

FIGURE 4. Shape of the TS derived from the plasma flow directions.

The IBEX results in Figure 2 provide a new view of the heliosphere; the ribbon region may represent the symmetry plane for the higher pressure regions and thus flow may be away from the ribbon, not the nose, which could better fit the data. Alternatively, the ribbon may be due to a line-of-sight selection effect for secondary ENAs born in the outer heliosheath from solar wind pickup ions gyrating around interstellar magnetic lines [Heerikhuisen et al., 2010].

Complicating this picture is the large latitudinal speed gradient associated with solar minimum, with high-speed, low-density flows at higher latitudes. We think that V2 was in the transition region between fast polar coronal hole flow and slow equatorial solar wind beginning just before the TS crossing [Richardson and Wang, 2010] and that corotating interaction regions (CIRs) were driving the variability in this region [Roelof et al., 2010], although TS motions may also play a role. This hypothesis explains a 30% decrease in solar wind flux observed before the TS and could explain differences among V1 flows, V2 flows, and model results. Ulysses observed the transition from low to high-speed flows at latitude 28°S in 2008, so V2 (now at 29°S) should be near this transition region. If V2 were moving into regions of higher-speed flow, the con-

stant V_R observed could result from a balance between the latitudinal speed increase and the expected slowdown across the heliosheath. Models which incorporate time dependent changes in the solar wind source and HCS tilt can reproduce the constant V_R observed by V2 because of this effect [Pogorelov et al., 2010].

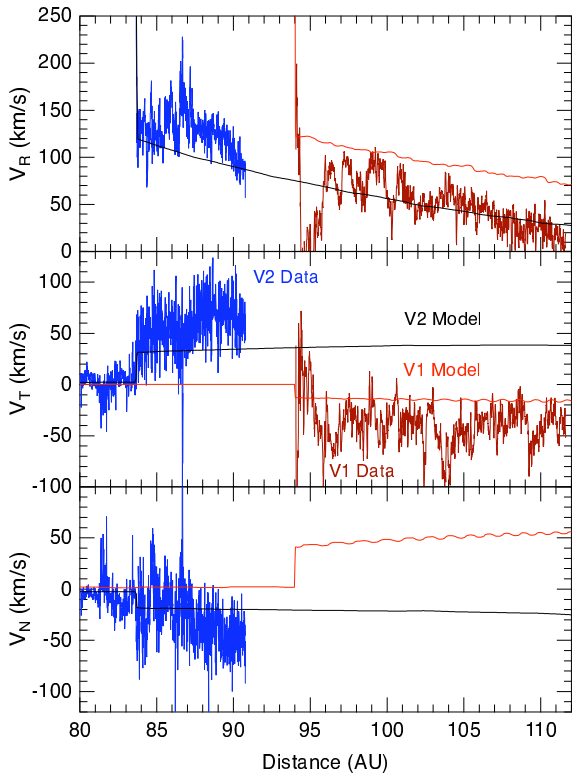

FIGURE 5. Plasma flow velocity components (V_R, V_T, V_N) in the heliosheath measured at V2 by the PLS instrument (blue) and estimated from the V1 LECP 53-85 keV ion data (dark red). Model predictions are shown for V1 (light red curve) and V2 (black curve).

3.2.1 Future Tasks

• Discover how the heliosheath plasma and flows evolve as V2 moves through the heliosheath. We expect

a) continued decrease of the radial speed and increased flow deflection as V2 nears the HP

b) A decrease in radial flux due to plasma moving tailward; the density may decrease significantly if a plasma depletion layer were observed ahead of the HP.

• Observe the effect of solar cycle changes in the heliosheath; collaborate with modellers to understand how the solar minimum conditions affect the observed speed profiles.

• Compare these data with model predictions to understand the flow pattern in the heliosheath and the direction of the interstellar magnetic field.

• Compare Voyager in situ data with the global IBEX ENA observations to determine the TS and heliosphere shape.

• Incorporate the new IBEX results into models for comparison with the Voyager data.

3.3 Large-Scale Structure of the Magnetic Field in the Heliosheath

Figure 6 shows an overview of the magnetic field strength and direction observed by V1 in the heliosheath. The average field strength is 0.11 nT with a standard deviation of 0.05 nT. Models of the heliosheath predict that the plasma speed will decrease with distance which will cause B to increase as V1 and V2 approach the heliopause [Parker, 1961, Axford, 1972; Nerney et al., 1991; 1993; Pauls and Zank, 1996; 1997]. In particular, the speed must go to zero at the nose of the heliopause. These stronger magnetic pressures might in turn modify the flow by driving an azimuthal (field-aligned) flow of plasma away from the nose. Contrary to these predictions, Voyager 1 observed a decrease in B in the heliosheath from 2005.0 through 2008.8 as shown by Figure 7 [Burlaga et al. 2009a]. This surprising result is probably a consequence of the decrease in B observed in the solar wind in the inner heliosphere. The magnetic field strength at 1 AU decreased from 6 nT during 2005 to near 4 nT in 2008 and the solar wind speed V at the latitude of V1 increased [Wang and Sheeley, 2009]. According to Parker's model [1963], B at large distances from the Sun is proportional to B at 1 AU and inversely proportional to V. Correcting for these solar variations, Burlaga et al. [2009d] find that B in the heliosheath did increase from 2005.0 to 2008.82 with a radial gradient of $0.017\text{nT/AU} \leq \text{grad B} \leq 0.0055$ nT/AU, consistent with model predictions.

The 3D MHD simulations of Linde et al. [1998] and Opher et al. [2003; 2004] predict that magnetic ridges form near the heliopause in conjunction with a slowing of the plasma flow. If these ridges were present, they would affect the dynamics of the flow and provide scattering sites for particle acceleration. The Voyager spacecraft will observe whether these magnetic ridges exist and if they were associated with a deceleration of the heliosheath flow.

During the declining phase and minimum of the current solar cycle, the latitudinal extent of the HCS decreased. Figure 7 shows the HCS location at the V1 and V2 locations computed by Wang and Sheeley [see Burlaga et al., 2009d] based on observations of the solar magnetic field. Their model predicts that the maximum latitudinal extent of the HCS drops below the latitude of V1 at 2006.33 and that V1 should observe unipolar fields throughout 2008. Figure 6 shows that

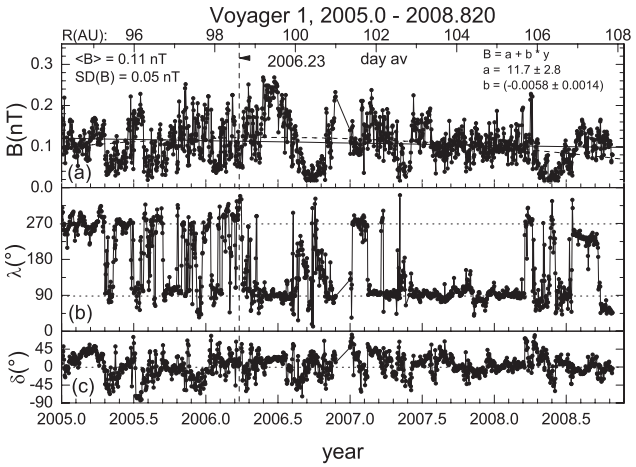

FIGURE 6. Daily averages of the magnetic field strength B, azimuthal angle λ, and elevation angle δ from 2005.0 to 2008.82. The line in panel (a) is a linear least squares fit to the data and the dashed curve is a parabolic fit.

V1 did observe predominantly "toward" polarities ($\lambda \approx 90°$) after 2006.33.

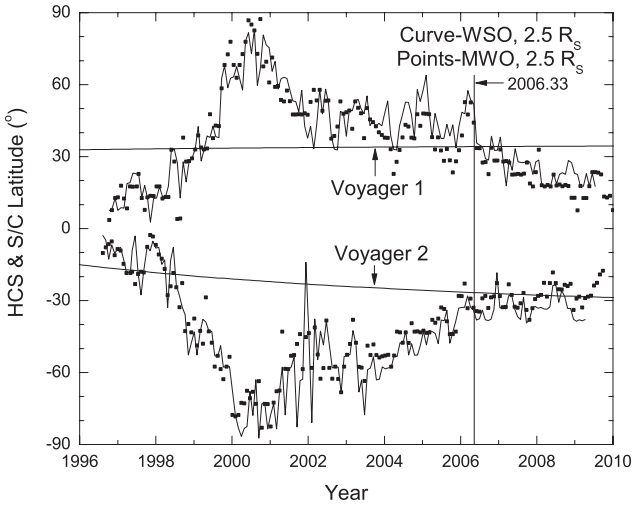

FIGURE 7. The maximum and minimum latitudinal extents of the heliospheric current sheet as a function of time computed from the "radial model" with the source surface at 3.25 solar radii with data from the Wilcox solar Observatory and the Mount Wilson Observatory. The latitudes of V1 and V2 are shown by nearly straight lines.

Figure 6 shows that V1 did observe some "away" polarities ($\lambda \approx 270°$) during 2008. Note, however, that the magnetic field direction cannot be measured accurately when B < 0.05 nT and when δ is large, so that some of the "away" polarities during 2008 might be artifacts. But the observations of "away" polarities from 2008.5 to 2008.7 are real. Pogorelov et al. [2010] predict that northward flow in the northern hemisphere of the heliosheath displaces the HCS northward even though the maximum HCS latitude decreased in the supersonic solar wind. This northward motion is due to the gradient in pressure of the interstellar magnetic field [Opher et al., 2006; 2007]. The occasional segments of away polarities observed by V1 during 2008 could be manifestations of the predicted northward flow in the northern hemisphere of the heliosheath as shown by the cover figure [Pogorelov et al., 2010]. Unfortunately, the northward component of the flow in the heliosheath is not measured by V1.

3.3.1 Future Tasks

• Examine the characteristics of the B in the heliosheath under solar minimum conditions when V2 and V1 are measuring flows from the polar coronal hole regions.
• Investigate the radial gradients of B in the heliosheath.
• Determine if magnetic ridges form in the heliosheath.
• Describe the large-scale fluctuations of B in the heliosheath and how they change with the solar cycle.

3.4 Evolution of the Heliospheric Current Sheet in the Heliosheath

Since the Voyagers measure data at only two points, we must use models and IBEX data to understand the global evolution of the HCS shape. Pogorelov et al [2010] solve the ideal MHD system using a two-fluid model for the interstellar neutrals. The cover figure shows the distribution of B in the plane formed by the V1 and V2 trajectories. The model is for a 20° tilt between the Sun's rotational and magnetic axes. The flow at V1 deflects northward at the TS and carries the HCS northward, so the latitudinal extent of the region of alternating magnetic polarities increases. This poleward motion of the HCS is not as pronounced in the V2 direction because the solar wind flow at V2 is primarily in the azimuthal direction. The model is used to calculate B along the V1 trajectory and derive a radial B gradient of 0.021 μG/AU, consistent with the range 0.017-0.055 μG/AU observed by V1 (see Section 2.2 and Burlaga et al. [2009d]).

3.4.1 Future Tasks

• Compare model predictions for the location of the HCS with V1 and V2 observations of HCS crossings.
• Study how the sector structure and boundaries change as solar activity and the HCS tilt increase.

3.5 Variations over Three Solar Cycles

McComas et al. [2006] examined the solar wind during Ulysses' second orbit and found that the stream structure was remarkably different and more variable than during Ulysses' first orbit. McComas et al. [2008] analyzed the solar wind observations from Ulysses third orbit and show that the fast solar wind was significantly less dense, cooler, slightly slower, and had less mass and momentum flux than during the previous solar minimum. These combined observations indicate significant, long-term variations in the solar wind output from the entire Sun. The long-term trend toward lower dynamic pressures means that the average heliosphere has been shrinking and that the heliopause will start to move inward toward V1 and V2.

Pogorelov et al. [2010] use Ulysses data to calculate steady state solar wind conditions corresponding to the first and third Ulysses pole-to-pole flybys. On the basis of Ulysses data, the latitudinal extent of the slow wind was chosen to be 20° for the first orbit and 27°S, 37° N for the third orbit. Figure 8 shows the distributions of the plasma density in the plane created by the V1 and V2 trajectories. For the 1996 minimum (see top of Figure 8), V1 was in the fast wind while V2 was in the transition region from slow to fast solar wind. During the current solar minimum, the latitudinal extent of the slow wind in the southern hemisphere is smaller than that in the northern hemisphere (23.4°S vs. 31.3°N). V1 is in the slow wind, although close to the boundary. These model results show that the heliosheath flows and thickness change dramatically on time scales of a solar cycle and from solar cycle to solar cycle, and that the configuration at a given time depends of the time history of the solar wind.

3.5.1 Future Tasks

• Identify the effects of solar cycle variations on the heliosheath magnetic field and plasma as the Voyagers observe the change from solar minimum to solar maximum conditions.

3.6 Pickup Ions and Suprathermal Spectra

Downstream of the TS, the LECP and CRS instruments on V1 and V2 observed spectra with suprathermal ion tails that have nearly perfect V^{-5} power law velocity distributions from ∼30 keV to a few MeV, at which energy the modulated ACR spectra begin to dominate. Recently, instruments on IBEX [McComas et al. 2009] and on Cassini [Krimigis et al. 2009] measured ENAs, which are created from pickup protons in the heliosheath, in the energy range of ∼0.1 to 45 keV.

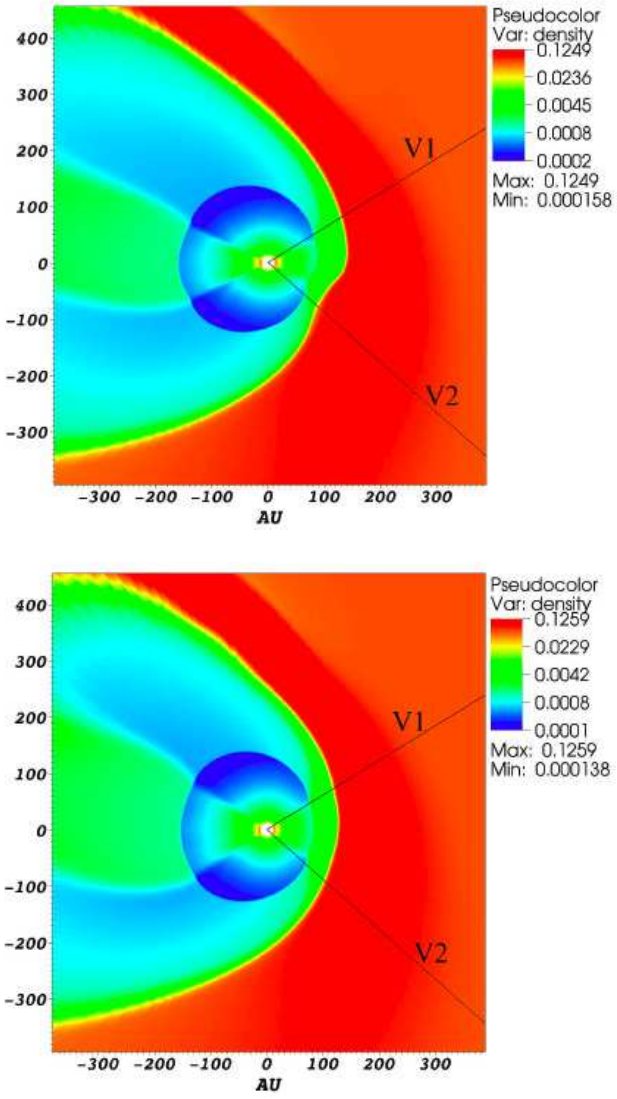

FIGURE 8. Plasma density distribution in the V1/V2 plane for (a) the 1996 solar minimum (top) and (b) the current solar minimum (bottom). The straight black lines are the spacecraft trajectories.

Much of this energy range (5-30 keV) is not observed by the V1 and V2 instruments. Using the method described in Krimigis et al. [2009], the line-integrated ENA spectra can be converted to average pickup proton spectra in the heliosheath as shown in Figure 9.

Pickup protons in the ENA emission region of the heliosheath (∼50 AU in width) would carry most of the pressure (∼8×10^{-13} dyne/cm^2) with the suprathermal V^{-5} power law tails close behind (∼4×10^{-13} dyne/cm^2). The dominant pickup ions are those created in the supersonic solar wind and then heated at the TS according to the Rankine-Hugoniot relations [Fisk et al., 2006]. Other pickup ions sources are charge exchange collisions of the heliosheath so-

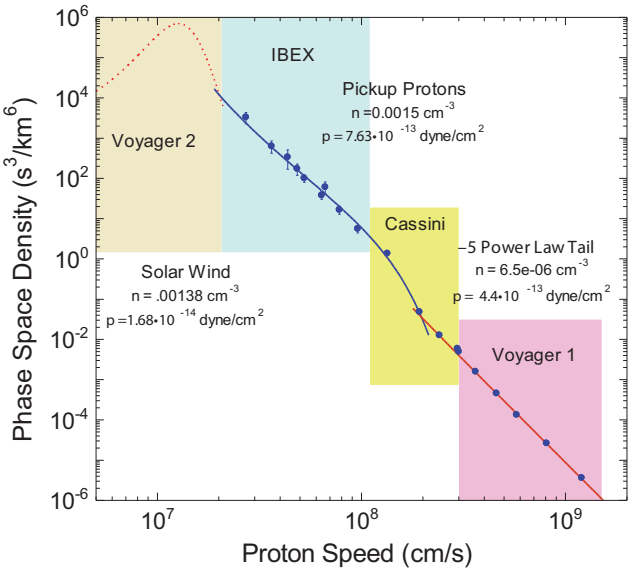

FIGURE 9. Composite velocity distribution in the heliosheath showing the long-term averaged solar wind thermal component measured by V2 (dotted curve), the V^{-5} suprathermal tail measured by V1 (red curve), and the pickup protons (blue curve) derived from IBEX and Cassini. The thermal solar wind pressure is only a few percent of the total pressure.

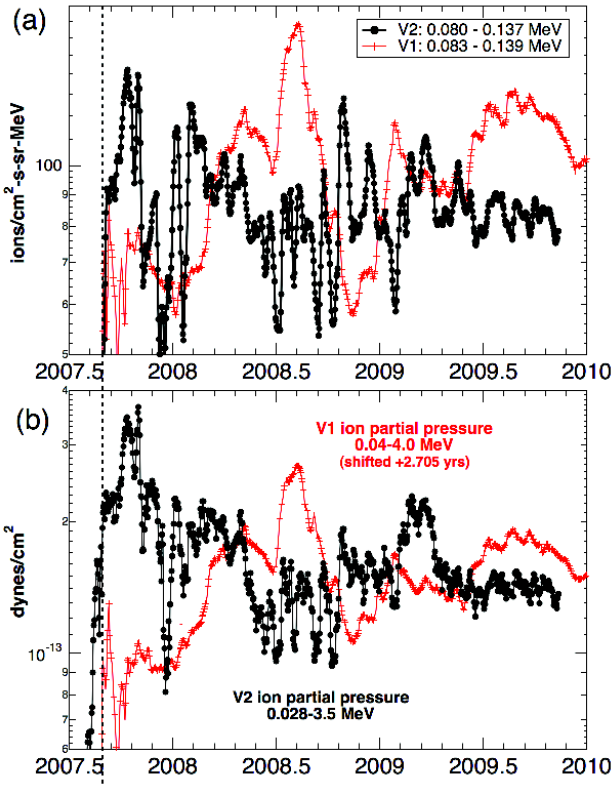

FIGURE 10. (a) Daily intensities of 0.08-0.14 MeV ions at V2 and V1. (b) Partial pressure of suprathermal heliosheath ions with energies 0.028-3.5 MeV at V2 and 0.040-4.0 MeV at V1.

lar wind protons both with interstellar neutrals and with the ENAs produced from charge-exchange of the supersonic solar wind with the interstellar gas. The Voyager measurements of the local plasma parameters and the suprathermal V^{-5} power law tails combined with the IBEX and Cassini observations of ENAs that provide a global picture of line-of-sight averaged velocity distributions of both pickup ions and the low energy portions of the tails contribute immensely to the understanding of the physical characteristics and dynamics of the heliosheath.

3.6.1 Future Tasks

• Document how the suprathermal tails change with distance from the TS along two widely separated paths through the heliosheath.
• Compare the ENA-derived pickup ion and low-energy tail distributions at the V1 and V2 locations to provide information on the spatial variations of pickup ion pressure and the thickness of the heliosheath.

3.7 Formation and Propagation of Perturbations through the Termination Shock to the Heliosheath

A puzzling feature of the LECP ion data in the heliosheath is that intensity variations measured at V1 and V2 are very different. Figure 10 shows V1 and V2 0.08-0.14 MeV ion intensities and partial pressures from their first 2.5 years in the heliosheath. Although V1 and V2 intensity levels are comparable, the time scales of intensity fluctuations are not. V2 ion intensities and partial pressures have had continuous quasi-periodic (12-35 day) variations with amplitudes from 5-25% since crossing the TS [Decker et al., 2009; Roelof et al., 2009]. These variations were not seen at V1. These variations may extend to the core of the heliosheath pickup ion population (lower in energy by a factor of ∼10 relative to the lowest measured energy of 28 keV) which carries the bulk of the plasma pressure.

These quasi-recurrent heliosheath ion variations could be produced by solar wind variations causing enhanced TS injection or acceleration, by re-acceleration of low-intensity suprathermal seed ions embedded in remnant CIRs at the TS, or some combination thereof. Populations of energetic ions and electrons accelerated or trapped when CIRs were closer to the sun may provide a quasi-recurrent seed population that can be re-accelerated at the TS and in the heliosheath [Rice 2000, Decker et al., 2001]. The quasi-periodic vari-

ations may be driven by large-scale, quasi-recurrent pressure variations in the solar wind at the heliolatitude (29°S) of V2. If the quasi-periodic V2 ion intensity variations were driven by solar wind pressure variations at 29°S, then the likely sources are high-speed solar wind streams from the equatorward extensions of polar coronal holes [Nolte et al., 1976]. The resulting stream-stream interactions produce pressure enhancements. Propagation of the corotating interaction regions (CIRs) and evolved merged CIRs out to 100 AU is a complex process [Burlaga et al., 2003a;b]. From an observational point of view, the existence of V2 ion intensity variations may provide evidence that quasi-recurrent solar wind pressure variations disturb the TS, even though velocity variations in the solar wind have damped out.

The V2 0.08-1.4 MeV ion intensity is plotted in Figure 11; the intensity variations change their character roughly every 6 months. The potential-field source-surface model synoptic coronal hole plots produced by the Global Oscillation Network Group (GONG) can be used to determine if CIRs were present at mid-latitudes (see the color plots in Figure 11). The highest closed field lines (blue) are those with vanishing radial component just below 2.5 solar radii; their loop tops are identified with the HCS (black line). The polarities of open flux regions (coronal holes) have footprints in the photosphere shown by the solid colors: green is positive, red is negative, and white areas have low-lying, closed field lines. The equatorial extensions show up as equatorward notches in the polar coronal hole boundaries. Well-developed high-speed streams near the sun are expected from only the larger equatorial extensions (>30°) that are clearly unipolar (i.e., green or red, but not white). The character of the V2 ion intensity variations was different in epochs A, B, C, and D defined in the upper panel of Figure 11. Allowing ∼1 year for the changes in the mid-latitude solar wind to propagate from the sun to the TS, sequential Carrington rotation (CR) plots were partitioned into 6-month groups (epochs A',B',C',D') that are one year earlier than the V2 epochs (A,B,C,D). The changes in the equatorial extensions of the southern polar coronal hole are consistent with the formation of strong mid-latitude CIRs near 1 AU that might produce pressure disturbances at the TS, thus generating the intensity variations in the energetic ion populations in the heliosheath observed at V2 (29°S). The absence of well-developed equatorial extensions in the boundary of the northern polar coronal hole is consistent with the absence of any significant energetic ion intensity variations at V1 (34°N). For period E, the equatorial extensions were larger in the north and faded in the south, and these Carrington rotation maps were used to predict the heliosheath ion time-intensity variations for the 2009-2010 V1/V2 data. The most recent V2 data show a reduction in the variations of the ∼100 keV ion intensities beginning in May 2009 and persisting through October 2009. V1 ion intensities are now starting to show noticeable variations. This confirmation of the prediction of Decker et al. [2009] and Roelof et al. [2009] supports the hypothesis that solar wind stream-stream interactions originating from equatorial extensions of polar coronal holes produce disturbances within the heliosheath downstream from the mid-latitude TS.

3.7.1 Future Tasks

• Determine how different solar wind flows are modified by the TS and by propagation within the heliosheath.
• Determine the effects of extensions of the polar coronal holes on flows, magnetic fields, and energetic particles in the heliosheath.
• Determine the nature and origins of fluctuations of the intensities of energetic particles as a function of changing solar activity.

3.8 Turbulence, Fluctuations, and Small-Scale Structures

One of the surprises observed by V1 in the heliosheath is the large-amplitude fluctuations in B at scales of several hours down to minutes. This variability at small scales is often referred to as "turbulence" owing to its complexity. However, basic turbulence properties such as the inverse cascade and the spectral structure and exponents have not been established for the heliosheath turbulence owing to the large daily data gaps.

The turbulence observed by V1 in the heliosheath is highly compressible with large fluctuations in B, in contrast to the nearly constant B observed in the turbulence in the solar wind near 1 AU. The turbulence in the heliosheath is a mixture of coherent and random structures. V1 observed nearly discontinuous changes, quasi-periodic changes, magnetic holes and magnetic humps, and other very complex structures in the heliosheath turbulence [Burlaga et al., 2006a]. Voyager 2 observed a similar type of turbulence during the first several months after it crossed the TS [Burlaga et al. 2009b,c].

The V2 plasma observations are particularly important for understanding the turbulence and its implications. Measurements of the speed are needed to estimate distances and lengths corresponding to temporal changes in the coherent structures observed in B. Jumps in 48 sec averages of B are frequently observed in association with these coherent structures. From the duration of the jumps and the measured speeds, one can estimate that the characteristic length scales were

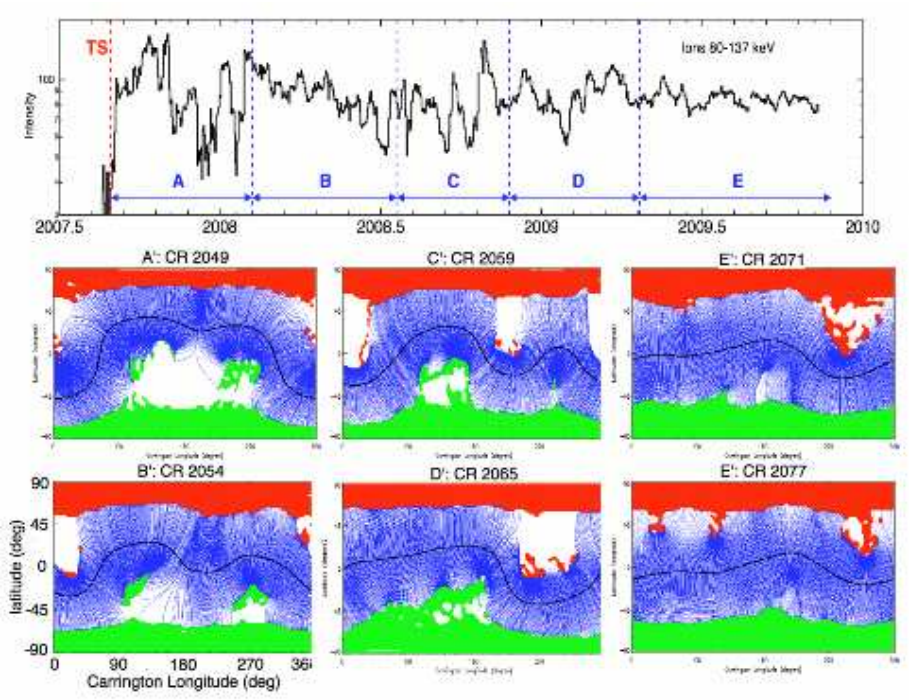

FIGURE 11. Upper: Daily averages of V2 0.08-0.14 MeV ion channel intensity. Lower: Color plots of one representative GONG CR map for periods A-E. CR numbers and associated time periods are: A', CRs 2047-2051, 10/0706-12/06/06; B', CRs 2052-2057, 2064-2069, 12/15/07-04/29/08; E', CRs 2070-2081, 05/27/08- 03/22/09. Gradual withdrawal of the equatorward extension of the southern polar coronal hole is consistent with the predicted and observed reduction of ion intensity fluctuations at V2 (E,E').

of the order of 150,000 km, which is likely related to the gyroradius of pickup protons. Given more refined theories of these coherent structures, it might be possible to use these observations to derive the effective temperature of the pickup protons in the heliosheath. Currently, we can only say that the pickup proton temperature behind the TS is greater than 2.5×10^6K and less than 4×10^7K [Burlaga et al., 2009c].

Figure 12 [Burlaga et al., 2009c] shows 48 sec averages of B observed by V2 behind the TS from day 245 - 301 of 2007. B varies by a large amount relative to the average B over a few hours, in some cases ranging from 0.02 nT to 0.25 nT. The turbulence is highly compressible and the fluctuations in B are highly nonlinear. The time series of 48 second averages of B in Figure 12 shows no obvious evidence of order. However, the time series of increments of magnetic field strength dBm = B(t + $2^m \times$ 48s) - B(t)) exhibits remarkable order. Figure 12 shows the increments of B at $2^4 \times$ 48s = 768 s intervals (dB4) measured by V2 and indicates that the turbulence is intermittent at this scale. Figure 13 shows that the distribution of the points dB4(t) at this scale is symmetric and has a large tail. The distributions of increments of B, dBm, at scales from 48 s to 6.8 hours (m = 1 to 9) are all symmetric and relatively simple. The solid curves in Figure 13 are fits of the observed distribution functions to the "symmetric Tsallis distribution" of nonextensive statistical mechanics [Tsallis, 1988; Burlaga et al. 2006b, 2007], which is the same as the q-Gaussian distribution associated with the generalized central limit theorem. Thus, the structure of the turbulence in the TS observed at small scales by V2 is in fact highly organized and described in part by a function that has a physical and mathematical meaning and which has found applications in many nonlinear, quasi-equilibrium systems.

It is important to understand the nature and origin of the turbulence in the heliosheath as it relates to the dynamics of the plasma and propagation of energetic particles. This understanding is likely to have applications to compressible MHD turbulence in other astrophysical systems. The q-Gaussian distributions observed in the V2 data are related to the intermittency of the turbulence. This relation means that the q-Gaussian distributions are derived from a relatively small number of points in the tails of the distributions. The magnetic field observed in the heliosheath by V1 and V2 thus far is very weak, ∼0.1 nT, which is comparable to the highly variable spacecraft magnetic field. The data set also has noise spikes from a variety of sources that must be carefully removed. Nevertheless, with sufficient care and effort it is possible to produce

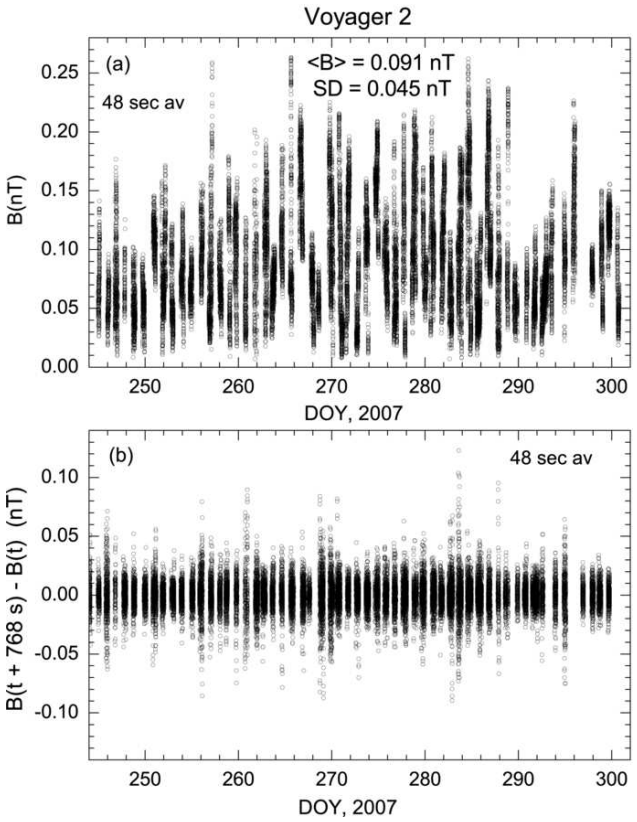

FIGURE 12. 48 s averages of B behind the TS (a) and increments of B at 768 s intervals (b) measured by V2.

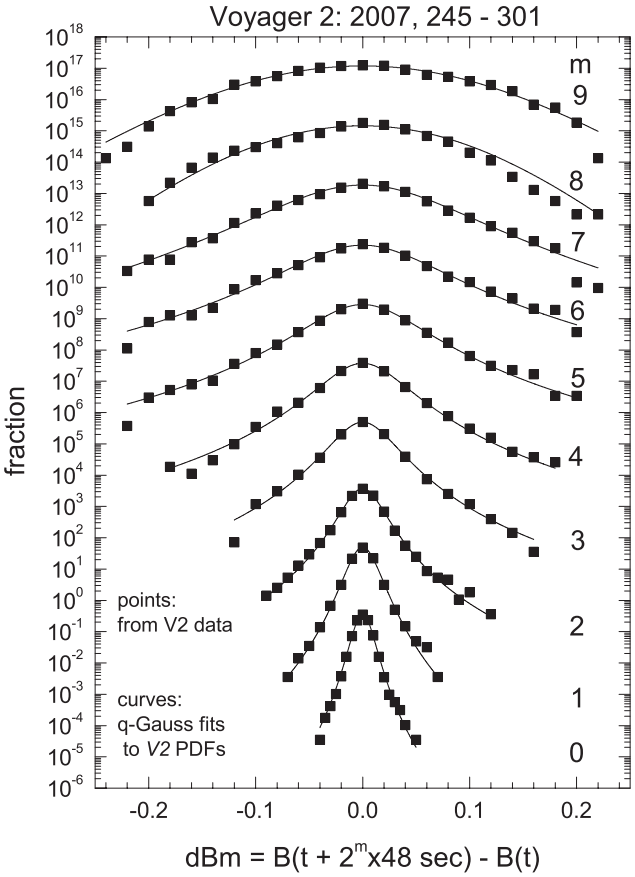

FIGURE 13. The observed distributions of increments of B (dBm) at intervals of $2^m \times$ 48 sec on scales from one minute to several hours. The curves are fits of the q-Gaussian distribution to the observed distributions.

sets of high-quality observations as shown in Figures 12 and 13. Since V1 and V2 will be moving into regions of increasingly strong magnetic fields, it should be possible to make more accurate observations of the turbulence, and to examine how it varies with distance and time in the heliosheath.

3.8.1 Future Tasks

• Understand the nature and origin of the compressible turbulence in the heliosheath.
• Determine how the nature of the turbulence in the heliosheath varies with distance from the TS, with variations in the solar cycle, and with various types of flows.

4. ANOMALOUS COSMIC RAYS

One of the major mysteries of the V1 and V2 termination shock (TS) crossings is that the source of anomalous cosmic rays (ACRs) was not observed at the TS. For nearly three decades the classical explanation of ACR origin was generally accepted: ACRs begin as interstellar neutral gas, which gets ionized in the heliosphere, picked up by the expanding solar wind, and accelerated to MeV energies at the TS [Fisk et al, 1974; Pesses et al., 1981]. However, when V1 and V2 crossed the TS the ACR He energy spectrum remained heavily modulated. The observed spectrum did not resemble the expected ACR source spectrum, a power-law at low energies with a roll-off at higher energies [Stone et al., 2005, 2008]. More will be learned about both the source location and the acceleration mechanism of ACRs over the next three years as the two Voyager spacecraft probe 10 AU further into the heliosheath and the onset of solar activity leads to increased ACR modulation.

Figure 14 shows the observed ACR He spectra at V1 in the heliosheath for five 52-day periods separated by 1 year. Note that the low-energy, below ∼1 MeV/nuc, component in the observed spectra (left panel) was accelerated at the shock and has changed very little in the last four years. These ions were discovered by Voyager and are called TSPs (Termination Shock Particles). The TSPs form when the core pickup ions, not

the suprathermal tail of the distribution, get accelerated at the TS [Giacalone and Decker, 2010]. The acceleration of these particles is responsible for the slow down of the solar wind observed as V2 approached the TS in 2007 [Florinski et al., 2009]. The TSP part of the energy spectrum observed by V1 and V2 is likely the same energy spectrum produced at the TS, which is then convected to the spacecraft with little modification. If few transients impact the shock, the TSP energy spectrum would be fairly stable, as has been observed at V1 for the last four years.

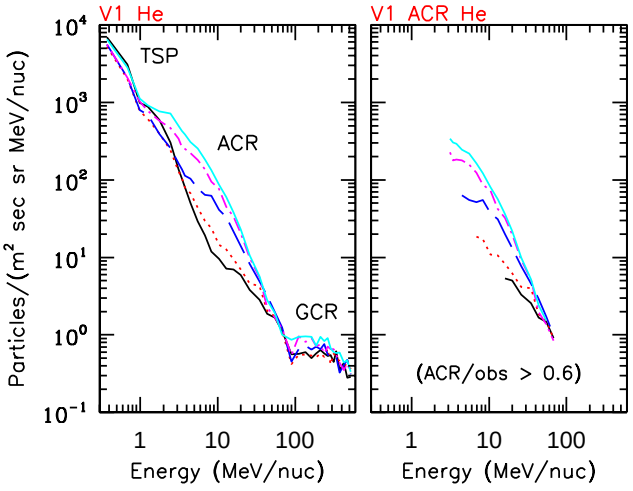

FIGURE 14. (left) Energy spectra of He at V1 for five 52-day periods from 2005/209-260 to 2009/209-260 (the intensity at 10 MeV/nuc increases with time). (right) ACR He spectra resulting from subtraction of estimated TSP and GCR spectra.

Above ∼100 MeV/nuc, the energy spectrum is dominated by galactic cosmic rays (GCRs) which are accelerated in the galaxy outside the heliosphere. Subtracting the TSP and GCR components, using power-laws to extrapolate into the ACR energy band, reveals the evolving ACR spectra shown in the right panel of Figure 14.

The ACR mystery has sparked several suggestions for the ACR source location and acceleration mechanism. In 2009 at least four different theoretical models for the origin of ACRs were advanced: Fisk and Gloeckler [2009], le Roux and Webb [2009], Lazarian and Opher [2009], and Drake et al. [2010]. This problem is a topic of interest to the community, with an international working group convened by ISSI to study this topic and special sessions organized at various meetings, such as at the SHINE workshop in 2009.

An earlier explanation that treats the problem globally was provided by McComas and Schwadron [2006]. They suggest that the blunt shape of the termination shock combined with a classical Parker spiral magnetic field (Figure 15) would result in acceleration that is more efficient towards the flanks of the heliosphere. This hypothesis still relies on the termination shock as the accelerator of the ACRs, but not at the locations where V1 and V2 crossed the TS. Variants of this idea, that ACR acceleration occurs primarily in the tail region of the TS or at hot spots along the TS, were also proposed by Kota [2008], Kota and Jokipii [2008], and Jokipii and Kota [2008].

Fisk and Gloeckler [2009] applied their combined theoretical and observational work related to suprathermal ions having phase space densities f that closely match a velocity power law spectrum with a -5 spectral index, i.e., $f \propto V^{-5}$ [Gloeckler et al., 2008] to ACR acceleration [Gloeckler et al., 2009; Fisk and Gloeckler, 2009]. Their theory uses a particular type of stochastic acceleration in the heliosheath and makes the prediction that the large majority of ACRs are accelerated near the heliopause, because that is where the pre-accelerated particles spend most of their time.

Two other papers discuss mechanisms which accelerate ACRs preferentially near the heliopause [Drake et al., 2010; Lazarian and Opher, 2009]. Lazarian and Opher [2009] suggest that fast magnetic reconnection is responsible for ACR acceleration. The ACRs gain energy at the expense of the magnetic energy that is lost during the field annihilation that takes place at magnetic field reversals. These reversals take place throughout the heliosheath, and in the solar wind as well, but close to the heliopause where the reversals become squeezed together the conditions for fast reconnection are improved.

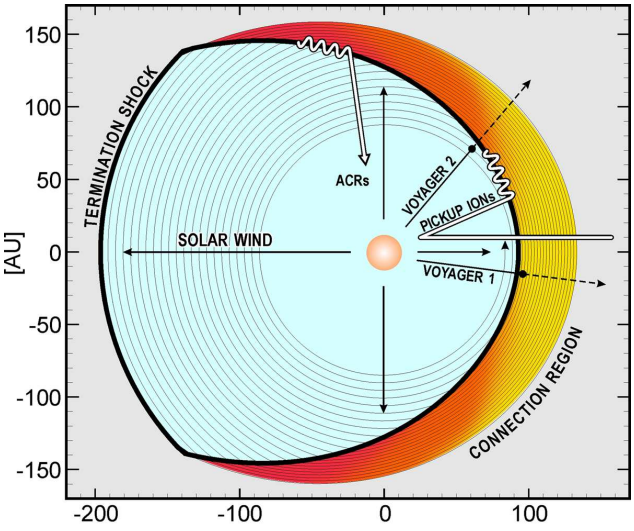

FIGURE 15. Schematic depiction of the heliosphere [from McComas and Schwadron [2006]) showing a blunt geometry that permits ACR acceleration at the TS in the heliospheric flanks.

Drake et al. [2010] ultimately rely on the same

global magnetic field reversals to provide the energy for their ACR acceleration mechanism. Their theory includes self-consistent acceleration of energetic particles within thinning current sheets where collisionless magnetic reconnection takes place. The acceleration of energetic particles arises from the contraction of magnetic islands and is a first order Fermi acceleration process, but occurs near the heliopause rather than at the TS.

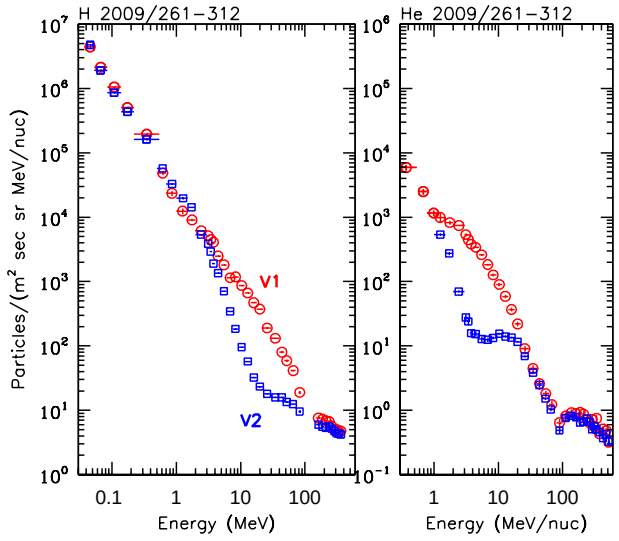

FIGURE 16. Energy spectra of H and He at V1 (red) and V2 (blue) for the period day 261-312 of 2009. The lowest five energy points in the left panel represent ion measurements without determination as to nuclear charge but are thought to be primarily H.

The Voyager measurements in the next few years will be crucial to discriminate amongst these theories or to provide evidence for an entirely different explanation. We can separate the effects of temporal changes and radial gradients by comparing the observed intensity gradient between the two Voyagers with the observed change at each spacecraft as they move outward at >3 AU/year. The gradients from the period day 261-312 of 2009 are illustrated in Figure 16, which shows the spectra of H and He at V1 and V2. For He at 4-20 MeV/nuc, where the ACRs are dominant at both spacecraft, the plot shows a clear gradient. At higher energies, no gradient is observed. Thus, we are probably observing the source intensity of ACR He above ∼30 MeV/nuc. We also note that the TSP spectra of H at V1 and V2 are similar, indicating that the acceleration conditions on the shock at locations 120 AU apart are similar.

The separation of spatial from temporal changes is illustrated in Figures 17 and 18. The time history of ACR He intensities at V1 in several energy bands is

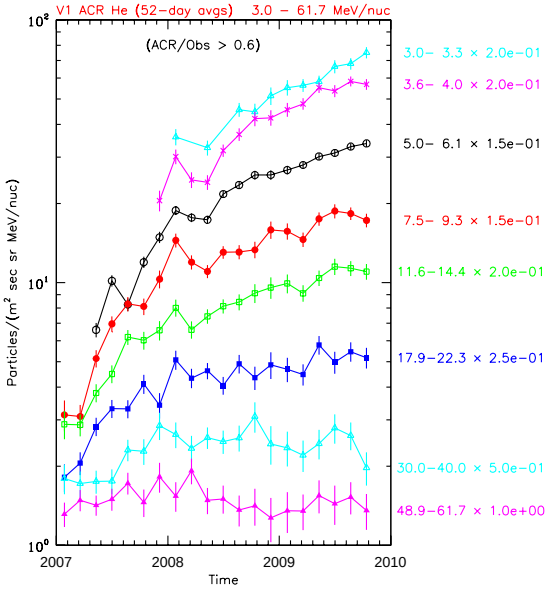

FIGURE 17. Fifty-two day averaged intensities of ACR He in several energy bands at V1 vs. time.

shown in Figure 17. Strong temporal changes in modulation were present before mid-2008, but since then the heliosheath has been in a quasi-steady state. In 2007, the rapid increase of intensities was observed at V1. This increase must have been primarily a temporal effect, since otherwise the radial gradients would be 32%/AU in the 11.6-14.4 MeV/nuc energy band, which is far greater than the radial gradient of ∼7%/AU between V1 and V2 observed at the same time (Figure 18). Thus we infer that this intensity change is due to decreasing ACR modulation beyond V1. Since mid-2008, however, the intensity rise at V1 is consistent with the V1/V2 gradient. Note that the intensities below ∼30 MeV/nuc still continue to rise, indicating that the V1 spacecraft has not reached the source region of these ACRs.

The tilt of the heliospheric current sheet at the Sun has recently decreased to near 10°, indicating that solar minimum conditions have finally arrived in the inner heliosphere. However, it takes about a year for this solar minimum magnetic field topology to reach the TS and another year to reach V1 which is 20 AU beyond the TS. Solar minimum conditions in the heliosheath will likely occur during the next two years as the current sheet tilt and quiet solar conditions are convected slowly beyond the TS.

Thus we expect that the next few years will be a quasi-steady period where we can measure the spatial gradients at different energies with good precision. If the ACR source were near the heliopause, we would expect that the gradient at low-energies might rapidly

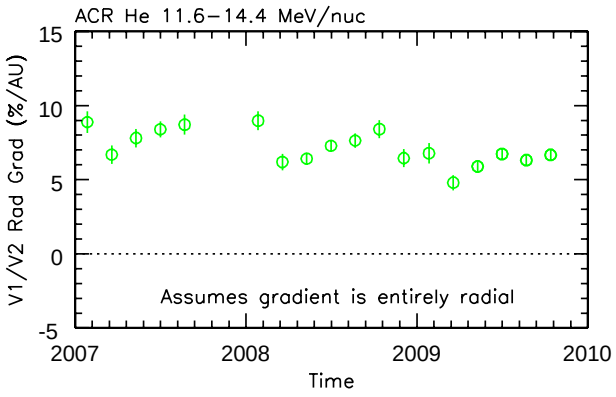

FIGURE 18. V1/V2 radial gradient of ACR He with 11.6-14.4 MeV/nuc vs. time.

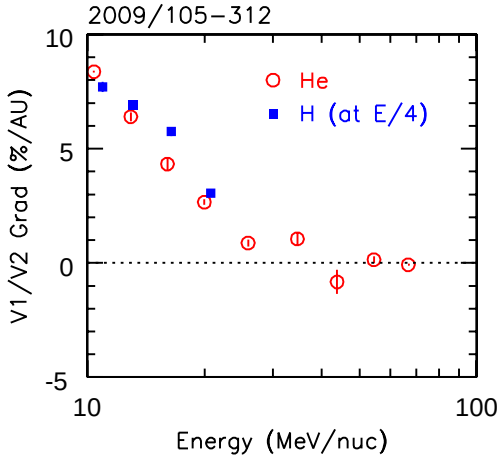

FIGURE 19. V1/V2 radial gradient of ACR He and ACR H vs. energy for the time period day 105-312 of 2009. The ACR H gradients are plotted at their energy in MeV divided by 4.

change as we approach it. However, if the ACR source were elsewhere, i.e., on the flanks of the TS, the lowest energy ACRs will remain modulated even at solar minimum conditions. In either case, there will be information from changes in the intensity gradient as solar minimum conditions are convected into the heliosheath.

Other observations are also important for investigations of the transport of energetic particles and for determining the composition of the gas in the local interstellar medium. For example, as seen in Figure 19, the energy dependence of the ACR He and ACR H gradients are similar if the H gradients are plotted at 1/4 of their energy. This scaling is due to the rigidity (R) dependence of the particle mean free pathlength, λ_{MFP}, [Cummings et al, 1984] and implies that $\lambda_{MFP} \propto$ R if the V1-V2 intensity gradient were a diffusive radial gradient. If the ACR source region were near the heliopause in the region of V1, we will measure the source spectra of all the ACR species.

4.0.1 Future Tasks

• Observe the evolution of the energy spectra of ACRs at V1 and V2, the intensity gradients between V1 and V2, and the gradients at each spacecraft as they move deeper into the heliosheath, and compare with models for the ACR source.
• Compare ACR spectra to estimate the rigidity dependence of the mean free pathlength in the heliosheath.
• Determine the composition of ACRs from measurements of their source spectra.
• Observe the effects of the transition from solar minimum to the onset of solar maximum on particle intensities and modulation in the heliosheath.
• Determine the nature, location, and frequency of magnetic reconnection in the heliosheath and near the heliopause and discover if it contributes to ACR acceleration.

5. BEYOND THE HELIOSHEATH

5.1 The source of radio emissions

Sporadic radio emissions at frequencies of 2 to 3 kHz have been observed by the two Voyager spacecraft for over twenty five years. These radio emissions primarily occur during the active part of the solar cycle and are believed to be generated when a strong outward propagating interplanetary shock interacts with the heliopause. Direction finding measurements [Kurth and Gurnett, 2003] have shown that the radio emission occurs along a line in the sky that is near to and almost parallel to the band of energetic ENA emissions recently detected by the IBEX and Cassini spacecraft (see Figure 20). Since radio emissions from interplanetary shocks tend to be generated most efficiently when the upstream magnetic field is nearly perpendicular to the shock normal, i.e., $B_n = 0$, Gurnett et al. [2006] suggested that the projection of the interstellar magnetic field onto the heliopause should be perpendicular to the observed line of radio emissions. This magnetic field geometry appears to be consistent with the interpretation of the ENA data which suggests that the interstellar magnetic field is oriented nearly perpendicular the band of ENA emission, as indicated by the white line in Figure 20.

Recent work suggests that reconnection might occur at the heliopause and play a role in the generation of the radio emission. Swisdak et al. [2009] show that

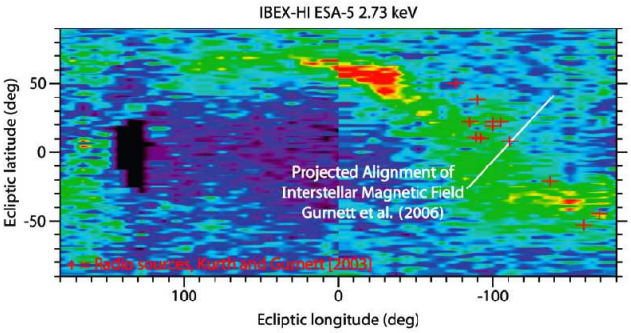

FIGURE 20. Comparison of the ENA fluxes observed by IBEX and the location of the radio emissions observed by Voyager.

the radio sources observed by V1 and V2 can be explained by reconnection at the heliopause between the draped interstellar magnetic field and the heliosheath magnetic field. They suggest that diamagnetic drifts in the high-beta plasma near the HP limit the reconnection to regions where the interstellar magnetic field is nearly anti-parallel to the heliospheric field. In their model, the location of the radio sources requires that the local interstellar magnetic field be oriented towards the north solar pole. Reconnection can produce both beams of electrons traveling at the electron Alfven speed [Cattell et al., 2005] and more isotropic populations at relativistic energies [Øieroset et al., 2002; Hoshino et al., 2001; Drake et al., 2006]. The electromagnetic decay mechanisms described in Cairns and Zank [2002] can then generate the 2-3 kHz radiation from these electrons. The model predicts stronger radio bursts in cycles 22 and 24 (near the next solar maximum) when the magnetic fields are anti-parallel at the nose.

Since solar activity is still very low following the recent solar minimum, no heliospheric 2 to 3 kHz radio emissions are currently detected by either spacecraft. However, as solar maximum approaches it is anticipated that the radio emission activity will again increase and provide further radio direction finding measurements for comparison with the IBEX and Cassini ENA data.

5.1.1 Future Tasks

• Determine whether fast magnetic reconnection plays a role in the production of radio emission by looking for reconnection signatures near the HP.

• Determine the nature, location, and frequency of magnetic reconnection in the heliosheath and in the heliopause.

5.2 The interstellar magnetic field

The local interstellar magnetic field is one of the key elements that control the interaction between the Solar System and the interstellar medium. Determining its strength and orientation is crucial because this field affects the shape of the heliosphere and the filtration of particles that stream into the heliosphere from the interstellar medium. When the Voyager spacecraft cross the heliopause, they will directly measure the orientation and strength of the interstellar magnetic field.

Measurements of the polarization of light from nearby stars suggest that the average field over spatial scales of parsecs is parallel to the Galactic disk [Frisch, 1996], but this technique gives no information on the local field direction. The backscattered solar Lyman-α radiation gave a field direction inclined 38°-60° with respect to the Galactic plane with the angle between the velocity of the interstellar medium and magnetic field assumed to be 30°-60° [Lallement et al., 2005]. This method relies on the assumption that the field is in a plane defined by the interstellar H and He flow directions as they penetrate the Solar System.

Opher et al. [2009] use the deflection of the solar wind plasma flows in the heliosheath and the observed difference in the TS locations at V1 and V2 to determine the magnetic field strength and orientation in the interstellar medium. They find the field strength in the local interstellar medium is 3.7-5.5 μG. The field is tilted 20-30° from the interstellar medium flow direction and about 30° from the Galactic plane, different from the plane found by Lallement et al. [2005]. This direction also differs from that of the large-scale field direction determined by Frisch et al. [2006], which could be a result of turbulence in the interstellar medium [Minter and Spangler 1996]. This difference could also be a consequence of a local distortion of the magnetic field in the solar vicinity [Frisch et al. 2009]. Heerikhuisen et al. [2010] show that fitting the IBEX ribbon with numerical models can help identify the interstellar magnetic field orientation.

5.2.1 Future Tasks

• Find a self-consistent explanation of the IBEX ribbon, the H deflection, and all the asymmetries detected by the Voyager spacecraft.
• When V2 crosses the HP, directly measure the in situ local interstellar magnetic field.

5.3 The Global Heliosphere and Beyond

V1 and V2 crossed the TS in December 2004 and August 2007 at 94 and 84 AU, respectively, and are approaching the HP. Ulysses observations [McComas et

al., 2008] show that the solar wind ram pressure this solar minimum is less (2.0 nPa compared to 2.6 nPa) than the previous two solar activity minimum periods. Thus the heliosphere has been shrinking and the heliopause will move inward toward the Voyager spacecraft. For steady-state gas dynamic solutions of the solar wind-LISM interaction problem, this would mean that all distances should be scaled by the square root of the ratio of these pressures (assuming the LISM properties have not changed between 2004 and 2007), resulting in a 14% decrease in the distance to the heliosphere boundaries. However, this scaling is only marginally correct for time-dependent solar wind. Moreover, there is a clear indication that an east-west asymmetry of the TS was consistent with the direction of propagation of energetic TS particles [Opher et al. 2006; Pogorelov et al., 2007; Decker et al., 2009].

Nevertheless, substantial efforts have been made recently to evaluate the TS asymmetries under the action of the interstellar magnetic field. Ideal MHD formulations of the solar wind-LISM interaction which did not include interstellar neutrals yielded large heliospheric asymmetries caused by the interstellar magnetic field [Opher et al., 2006; Pogorelov et al., 2004]. Charge exchange between ions and neutral atoms significantly decreases this heliospheric asymmetry, so that stronger interstellar magnetic fields are required to match the observed TS locations [Pogorelov et al., 2007; 2008; Opher et al., 2009]. The plane formed by the velocity and magnetic field vectors (V_∞ and B_∞) in the distant LISM is defined with a reasonable accuracy [Pogorelov et al., 2007; 2008] by the hydrogen deflection plane (HDP) formed by the velocity vectors of the neutral H flows in the unperturbed LISM and in the inner heliosphere [Lallement et al., 2005]. The angle between B_∞ and V_∞ is chosen so that the magnetic pressure produces the observed asymmetry of the TS. This angle cannot be too close to 0 or 90°. If the density of neutral hydrogen in the LISM were kept fixed while the LISM magnetic field strength B_∞ is increased above 4 μG, the model TS distance in the V1 direction will increase with respect to the TS distance in the V2 direction so that the model results are consistent with the observations [Pogorelov et al., 2007].

5.3.1 Where is the heliopause and what is its structure?

The ultimate goal of the Voyager Interstellar Mission is to observe the LISM. Both Vl and V2 are now in the inner heliosheath; how long must we wait for these spacecraft to reach the outer boundary of the solar system, the heliopause? The thickness of the inner heliosheath is likely different in the Vl and V2 directions and depends on the solar wind and LISM parameters. The current decline in solar wind pressure and activity is causing the heliosphere and the HP distance to shrink. Many numerical computations have been run to determine the width of the heliosheath and results range from 43-86 AU in the V1 direction and from 34-55 AU in the V2 direction [Pogorelov et al., 2007; 2008; 2009: Opher et al., 2007, 2008, 2009; Heerikhuisen et al., 2008; Washimi et al., 2009]. These estimates do not take into account the current decrease in the solar wind dynamic pressure, which should bring the HP 14%, or ∼15 AU, closer. Vl moves outward about 3.56 AU/yr and V2 move outward about 3.16 AU/year. These values give HP crossing times as early as 2015 for both V1 and V2.

5.3.1 Future Tasks

• Incorporate IBEX and Voyager data to improve and verify heliosphere models.
• On a longer time scale, observe the HP locations in the V1 and V2 directions and determine the asymmetry.

5.4 The structure of the heliopause

The heliopause (HP) is a tangential discontinuity that divides the interacting streams of the solar wind and local interstellar medium (LISM). The heliopause is thought to be subject to Rayleigh-Taylor instabilities driven and mediated by interstellar neutral atoms [Zank et al., 1996; Florinski et al., 2005]. Borovikov et al. [2008] identified a new form of instability on the flanks of the HP driven by hot neutral hydrogen atoms created by charge exchange of interstellar neutrals with hot heliosheath plasma. They show that secondary neutrals play an essential role in destabilizing the flanks of the HP. The time-dependent location of the HP and the termination shock and the influence of their excursions on the plasma distribution in the inner heliosheath create various waves in the subsonic solar wind flow in the heliosheath. Perturbations generated by the HP instability can affect the distribution of plasma in the inner heliosheath at shorter time scales than the time-scale of the instability as it develops near the stagnation axis. The characteristic time scale for the linear stage of the instability development is related to the charge exchange frequency, which was estimated by Florinski et al. [2005] to be about 2×10^{-8} in the heliosheath. This gives a time scale for instability growth of 1.6 years. However, the nonlinear growth time is considerably larger, ∼60 years, if we disregard very fine structures due to energy cascading to small vortices. These results suggest that Voyager is likely to travel through a structurally complex region with the width of about 20 AU in the vicinity of the HP.

This complex structure would not be due to solar wind variability, but to instabilities on the HP. Propagation of solar wind disturbances (GMIRs, etc.) should not create this kind of variability at the HP because solar wind disturbances have latitudinal/longitudinal extent much greater than 20 AU and these disturbances weaken significantly as they propagate from the TS to the HP. Time-dependent simulations based on solar cycle variations do not introduce this kind of structural, long-lived modifications to the HP [see Zank and Muller 2003; Scherer and Fahr 2003; Izmodenov et al. 2005; Pogorelov et al., 2009b]. The Voyager spacecraft could observed these precursors 5-6 years before the HP crossing; if these precursors are observed they would support the presence of these instabilities.

5.4.1 Future Tasks

- Look for HP precursors.
- Compare these precursors with model predictions.

6. GALACTIC COSMIC RAY MODULATION BEYOND THE TERMINATION SHOCK AND THE INTERSTELLAR COSMIC RAY SPECTRUM

The passage of V2 through the TS in late August of 2007 ushered in a new realm for the study of galactic cosmic rays and the effects of solar modulation in the outermost regions of the heliosphere. As of 2010.0, V2 is at 91 AU, 10 AU beyond the current estimated location of the TS and V1 is at 112 AU, 25-30 AU beyond the TS location. Solar activity remains at a historic low for the modern era. The interplanetary magnetic field at 1 AU is 28% below the "floor" hypothesized from the previous 4 solar minima, so the galactic cosmic ray intensity is at a maximum throughout the heliosphere. In the ensuing 2-3 years, before any solar activity increase in the new cycle is observed in the outer heliosphere, both Voyagers will have journeyed deeper into the heliosheath. This whole new unexplored region of solar modulation that is beyond the TS, but still under the influence of an outward flowing, magnetized solar wind, is now accessible for study. The interpretation of the cosmic ray gradient and time variation data will depend strongly on the extension of present modulation models to reflect the newly determined plasma and magnetic field data beyond the TS along with the unusual current conditions throughout the heliosphere.

The ultimate goal of these studies is to find the interstellar spectra at lower energies of all cosmic ray species, including primary nuclei such as H, He, C, O, Fe, secondary nuclei such as boron and nitrogen and, perhaps most interesting of all, galactic electrons. These spectra, as well as the charge and isotopic composition of these different species, can be accurately measured by the CRS experiment and contain a wealth of information about conditions locally and on a galactic scale. The plasma density, magnetic field, and the structure of the plasma turbulence on a large and small scale that determine the actual propagation (diffusion) of these particles throughout the galaxy will also be measured. Voyager now is evolving toward becoming a true interstellar probe, able for the first time to study astrophysical features of the galaxy that have been previously inaccessible to direct measurement.

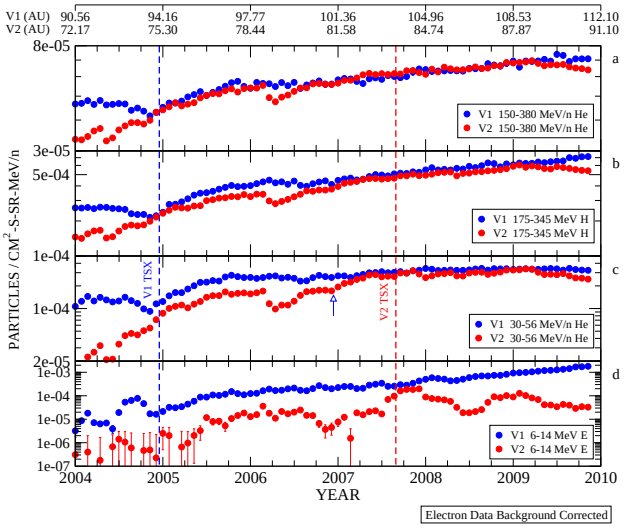

FIGURE 21. The intensity of GCR and ACR nuclei and electrons at V1 (blue) and V2 (red) for 2004 through 2009.

Cosmic ray electrons are an excellent example of astrophysical features that, because of Voyager, we can now study. These particles, through their synchrotron radiation in the galactic magnetic fields, are responsible for the galactic radio emission observed from ∼1 to >1000 MHz. The spectrum of galactic radio emission maps out the interstellar electron spectrum. This electron spectrum is predicted to match that observed by Voyager when it reaches the heliospheric modulation boundary. This process of matching and what is necessary to accomplish it will be an important new area of study that that crosses the line between solar physics modulation and galactic astrophysics propagation.

After the V1 termination shock crossing the >5 MeV/nuc ACR ions, the GCR ions and the electrons all rapidly increased in intensity. This increase is both temporal and spatial in nature and continues to the present. This continuing increase is most dramatic in the 2.5-175 MeV electron intensity (e.g., see Figure 21) and is a combination of spatial and temporal effects as

the electron intensity increases towards its LISM value. If it were solely spatial in nature, the radial intensity gradient in the heliosheath would be ∼20%/AU. The measured electron energy spectra (Figure 22) at ∼2009.5 has a slope of 1.67 and is a factor of ∼10 below the LISM spectra [Webber and Higbie, 2008]. At the present rate of increase this V1 spectrum will match the calculated LISM spectrum in 2012 when V1 will be at ∼120 AU.

Table 1. Intensity gradients in the heliosheath.

V1	2006.14-2008.92	% < LISM
150-380 MeV/n He	7.4%/yr	21%
145-244 MeV/n He	9.6%/yr	30%
180-350 MeV/n H	15.5%/yr	44%
30-56 MeV/n He	3.5%/yr	
6-14 MeV e^-	75%/yr	

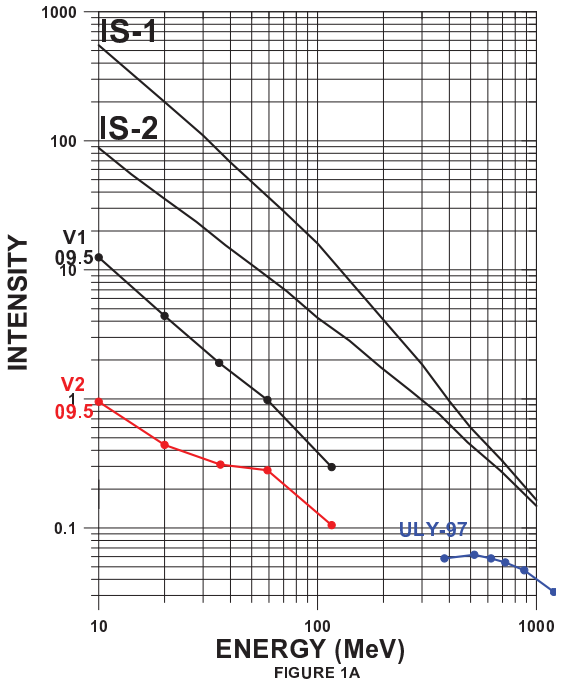

FIGURE 22. The electron spectra at V1 and V2 in mid-2009. The ULY-97 spectrum is from Ulysses during last solar minimum [Ferreira et al., 2000]. The model interstellar spectra (IS-1 and IS-2) reflect different assumed interstellar diffusion coefficients [Webber and Higbie, 2008].

The V1 time histories of 265 MeV/n GCR He and H, 43 MeV/n ACR He and 10 MeV electrons in Figure 21 show a consistent pattern from 2007-2009.9. The GCR and ACR ions have a steady intensity increase and a very small radial gradient. (<0.3%/AU). The large intensity increases in Table 1 must be predominantly temporal and not spatial. The rate of change of 265 MeV H (rigidity R=684 MV) is twice that of 265 MeV He (R=684 MV). A cross-correlation plot of 10 MeV electrons and 265 MeV/n GCR He shows a very close relation between these two components (Figure 23), which suggests that the very low rigidity electrons and the GCR He have followed the same path from the LISM to V1 in the heliosheath. Since the Axford-Cranfield effect should produce a strong magnetic field barrier at the nose and flanks of the heliosheath [Florinski et al., 2009], this observation poses a serious problem for understanding particle transport in the heliosheath. It is interesting to note that all 4 GCR components will approach their expected LISM intensity in about 3 years [Webber and Higbie, 2008]. The decreasing intensities of GCRs and high energy ACR He at V2 during 2009 is not understood.

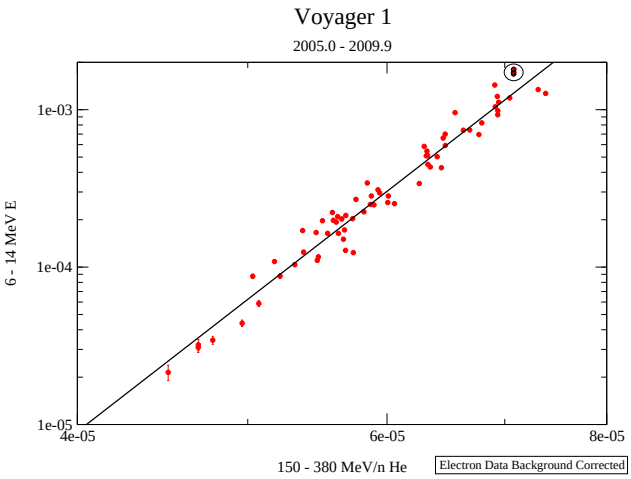

FIGURE 23. The correlation of the intensities of GCR He (150-380 MeV/nuc) and GCR electrons (6-14 MeV) for 2005 through 2009.

The continuing acquisition of cosmic ray data from the Voyagers in the heliosheath and the previous 36 years of data from Pioneer, Voyager, Ulysses, IMP and ACE have provided a comprehensive record of the spatial and temporal variations of galactic cosmic rays over several 11-year solar cycles in the heliosphere. This record provides the basis for more precise modeling of the overall solar modulation process in the heliosphere which is important to interpret such varied topics as (1) the comprehensive cosmic ray charge isotope data from the ACE spacecraft near Earth and (2) the long term changes observed in the 10Be ice core concentration and the relationship of these changes to both long term solar modulation and climatic changes.

7. SUMMARY

The Voyager spacecraft continue their epic journey of discovery, traveling through a vast unknown region of our heliosphere on their way to the interstellar medium. Both Voyagers are now traversing the heliosheath, with the first crossings of the HP and the first in situ observations of the interstellar medium still to come. These encounters could answer many basic, long-standing questions about the plasma and magnetic properties of the LISM, the nature of the TS and its role in the acceleration of the ACRs, the role of the heliosheath in GCR modulation, the spectra of low-energy interstellar GCRs, and the source and location of the heliospheric radio emissions.

Exploratory missions such as Voyager provide key tests of physical theories and also provide observational surprises which often lead to major advances in physical understanding. The continued ACR modulation in the heliosheath, the pre-shock slowdown and lack of heating of the thermal plasma at the TS, the low shock strength of the TS, and increases in the 6-14 MeV galactic electron intensities in the heliosheath are a few examples of observations forcing revisions to long-term hypotheses on particle acceleration. The combination of the IBEX ENA mapping and the Voyager in situ observations should lead to many advances on these fronts as well as to the understanding of the heliospheric-LISM interaction in a global sense.

The longevity of the Voyagers makes them ideal platforms for studying solar cycle variations in the heliosheath. Their distance make them ideal for studying the evolution of the solar wind, shocks, and cosmic rays. The interpretation of Voyager data is greatly enhanced by the ability to compare with data from Earth-orbiting spacecraft (Wind, ACE, SAMPEX, STEREO), Ulysses, and IBEX. These data make deconvolution of solar cycle, distance, and latitude effects possible. To further this intercomparison of data sets and to provide opportunity for the community to provide new insight into these observations, we strongly endorse Guest Investigator and Theory programs focusing on the outer heliosphere. Theory and multi-spacecraft comparisons are needed to provide the best understanding of the data Voyager provides. The Voyager Interstellar Mission provides a unique chance to study both temporal and spatial variations in the outer regions of our heliosphere and beyond and we should fully capitalize on this opportunity.

8. REFERENCES

Axford, W.I. (1972) in Solar Wind, edited by C.P. Sonett, J. Coleman, P. J., and J.M. Wilcox, pp. 609, NASA Spec. Publ.

Burlaga, L. F., et al. (2003a) Astrophys. J., 590, 554 .

Burlaga, L. F., et al. (2003b) J. Geophys. Res., 108, 8028.

Burlaga, L. F., et al. (2005) Science, 309, 202.

Burlaga, L. F., et al. (2006a) Astrophys. J., 642(1), 584.

Burlaga, L. F., et al. (2006b) Astrophys. J., 644(1), L83.

Burlaga, L. F., et al. (2007) J. Geophys. Res., 112, A07206.

Burlaga, L. F., et al. (2008a) J. Geophys. Res., 113(A2).

Burlaga, L. F., et al. (2008b) Nature, 454, 75.

Burlaga, L. F., et al. (2009a) Astrophys. J., 692(2), 1125.

Burlaga, L. F., and N. F. Ness (2009b), Astrophy. J. Lett., 703, 311 .

Burlaga, L. F., et al. (2009c) Astrophys. J. Lett. 691(2), L82.

Burlaga, L. F., et al. (2009d) J. Geophys. Res, 114 (A06106).

Borovikov, S. N. et al. (2008) Astrophys. J., 682, 1404.

Cairns, I. H., and G. P. Zank (2002), Geophys. Res. Lett., 29, 1143,

Cattell, C., et al. (2005) J. Geophys. Res., 110, A01211

Cummings, A. C., et al. (1984) Astrophys. J. Lett., 287, L99.

Decker, R. B., et al. (2001) Proc. COSPAR, Pergamon, New York, 11, 321.

Decker, R. B., et al. (2009) Shock Waves in Space and Astrophysical Environments, AIP Proc., in press.

Drake, J. F., et al. (2006) Nature, 443, 553-556, doi: 10.1038/nature05116.

Drake, J., et al. (2010) Astrophys. J., 709, 963.

Ferreira, S. E. S. et al. (2000) J. Geophys. Res., 105, 18305.

Fisk. L. A. et al. (1974) Astrophys. J. 190, L35.

Fisk, L. A., et al. (2006) Astrophys. J. 644, 631?637,

Fisk. L. A., and G. Gloeckler (2009) Adv. Space Res. 43, 1471.

Florinski, V., et al. (2005) J. Geophys. Res, 110, A07104.

Florinski, V., et al. (2009), Geophys. Res. Lett., 36, L12101.

Florinski, V., et al. (2010), SW12 proceedings, in press.

Frisch, P. C. (1996) Space Sci. Rev. 78, 213.

Frisch, P. C. et al. (2009) Space Sci. Rev., DOI 10.1007/s11214-009-9502-0.

Giacalone, J., and R. B. Decker (2010), Astrophys. J. 710, 91.
Gloeckler, G., et al. (2009) Space Sci. Rev., 143, 163.
Gurnett , D.A., et al. (2006), AIP Conf. Proc. 858, 129.
Heerikhuisen, J., et al.(2008) Astrophys. J., 682, 679.
Heerikhuisen et al. (1010), Astrophys. J. Lett., 708, L126.
Hoshino, M., et al. (2001) J. Geophys. Res., 106, 25979.
Izmodenov, V., et al. (2005) Astron. Astrophys., 437, L35.
Izmodenov, V. (2009) Space Sci. Rev. 143, 139.
Izmodenov, V., et al. (2008) Adv. Space Res. 41, 318.
Jokipii, J. R., and J. Kota (2008) in Particle Acceleration and Transport in the Heliosheath and Beyond?7th International Astrophysics Conference, G. Li et al., eds., American Institute of Physics, CP1039, 390.
Kota, J. (2008) Proc. 30th Internat., Cosmic Ray Conf., Merida, Vol. 1, 853.
Kota, J., and J. R. Jokipii (2008) in Particle Acceleration and Transport in the Heliosheath and Beyond - 7th International Astrophysics Conference, G. Li et al., eds., American Institute of Physics, CP1039, 397.
Krimigis, S. M., et al. (2009) Science, 326, 971.
Kurth, W. S. and Gurnett, D. A. (2003) J. Geophys. Res., 108, 8027.
Lallement, R. et al. (2005) Science 307, 1447.
Lazarian, A., and M. Opher (2009), Astrophys. J. 703, 8.
Le Roux. J. A., and G. M. Webb (2009) Astrophys. J., 603, 534.
Linde, T. J., et al. (1998) J. Geophys. Res. 103, 1898.
McComas, D. J., et al. (2006), Geophys. Res. Lett., 33, L09102.
McComas, D. J., and N. A. Schwadron (2006) Geophys. Res. Lett., 33, L04102.
McComas, D. J., et al. (2008), Geophys. Res. Lett., 35, L18103.
McComas, D. J. et al. (2009) Science, 326, 959.
Minter, A. H. and Spangler, S. R. (1996) Astrophys. J. 458, 194.
Nerney, S., et al. (1991) Astron. Astrophy., 250, 556.
Nerney, S., et al. (1993) J. Geophys. Res., 98, 15169.
Nolte, J. T., et al. (1976) Solar Phys., 46, 303.
Øieroset, M., et al. (2002) Phys. Rev. Lett., 89, 195.
Opher, M., et al. (2003) Astrophys. J., 591, L61.
Opher, M., et al. (2004) Astrophys. J. , 611, 575.
Opher, M., et al. (2006) Astrophys. J. Lett., 640, L71.
Opher, M. et al. (2007) Science 316, 875.
Opher, M. et al. (2009a) Space Sci. Rev., 143, 43.
Opher, M., et al. (2009b) Nature, 462, 1036.
Parker, E. N. (1961) Astrophys. J., 134, 20.
Parker, E. N., (1963) Interplanetary Dynamical Processes, Interscience, New York.
Pauls, H. L. and G. P. Zank, (1996) J. Geophys. Res., 101, 17081.
Pauls, H. L. and G. P. Zank, (1997) J. Geophys. Res., 102, 19779.
Pesses, M.E., et al. (1981) Astrophys. J., 246, L85.
Pogorelov et al. (2004), Astrophys. J., 614, 1007.
Pogorelov et al. (2006), Astrophys. J., 644, 1299.
Pogorelov et al. (2007), Astrophys. J., 668, 611.
Pogorelov et al. (2008), Astrophys. J. Lett., 675, L41.
Pogorelov et al. (2009a), Astrophys. J. Lett., 695, L31.
Pogorelov et al. (2009b), Astrophys. J., 696, 1478.
Pogorelov et al. (2010), in Proc. Solar Wind-12.
Richardson, J. D, et al (2008) Nature, 454, 63.
Richardson, J. D (2009) Geophys. Res. Lett., 36, L10102.
Richardson, J. D, and Wang, C. (2010) Astrophys. J. Lett, in press.
Rice, W. K., et al. (2000) Geophys. Res. Lett., 27, 509.
Roelof, E. C., et al. (2009) Solar Wind 12, AIP Proc., in press
Scherer, K., and Fahr, H. J. (2003) Geophys. Res. Lett., 30, 1045.
Scurry, L., et al. (1994) J. Geophys. Res., 99, 14811.
Stone, E. C., et al. (2005) Science 309, 2017.
Stone, E.C., et al. (2008) Nature 454, 71.
Story, T. R., and G. P. Zank (1995) J. Geophys. Res., 100, 9489.
Story, T. R., and G. P. Zank (1997) J. Geophys. Res., 102, 17381.
Swisdak, M., et al. (2003) J. Geophys. Res., 108, 1218.
Swisdak, M., et al. (2010), Astrophys. J., in review.
Tsallis, C. (1988) J. Stat. Phys., 52, 479.
Washimi, H. et al. (2010) AGU, Fall Meeting, abs. SH24A-04
Webber, W. R., and P. R. Higbie (2008) J. Geophys. Res., 113, A11106.
Whang, Y. C., et al. (1995) J. Geophys. Res., 100, 17,015.
Zank, G. P. et al. (1996) J. Geophys. Res., 101, 21639.
Zank, G. P., and Muller, H. R. (2003) J. Geophys. Res., 108, 1240.

9 TECHNICAL/BUDGET

9.1 Introduction

The Voyager Interstellar Mission (VIM) started in 1990 when the Voyager spacecraft were over twelve years old, having already returned a wealth of scientific information about the giant gaseous planets and the interplanetary medium between Earth and Neptune. The Voyagers are in their 33rd year of flight operations.

Voyager 1 is escaping the solar system at a speed of about 3.6 AU/year while Voyager 2 is leaving at about 3.3 AU/year. Power is the limiting lifetime consumable. The two spacecraft have power to continue returning science data from all plasma, waves and particles instruments until at least the year 2020. It is likely that at least one of the spacecraft could enter interstellar space while adequate power is still available. All other consumables are adequate for continued operations well past 2020.

9.2 The Voyager Spacecraft

Voyager spacecraft subsystems and instruments required for the interstellar mission are operating well and are fully capable of supporting the science mission through 2020 and beyond. Although both spacecraft are operating on some redundant hardware, with careful monitoring of spacecraft health, considerable functional flexibility still exists to operate a long duration mission. In the past year, several changes – described within the following text – have been made to extend functional life of several critical subsystems.

The identical Voyager spacecraft (Figure 24) are three-axis stabilized systems that use celestial or gyro referenced attitude control to maintain pointing of the high-gain antennas toward Earth. The prime mission science payload consisted of 10 instruments (11 investigations including radio science). Only five investigator teams are still funded, though data are collected for one additional instrument, the Ultraviolet Spectrometer (UVS). Active instruments and their status are described in Section 1: Introduction. The project's science investigators are listed in Table 1.

The entire Voyager 2 scan platform, including all of the platform instruments, was powered down in 1998. All platform instruments on Voyager 1, except UVS, have been powered down. The Voyager 1 scan platform was scheduled to go off-line in late 2000, but has been left on at the request of the UVS investigator (with the concurrence of the Science Steering Group) to investigate UV emission from the upwind direction. UVS data are still captured, but scans are no longer possible.

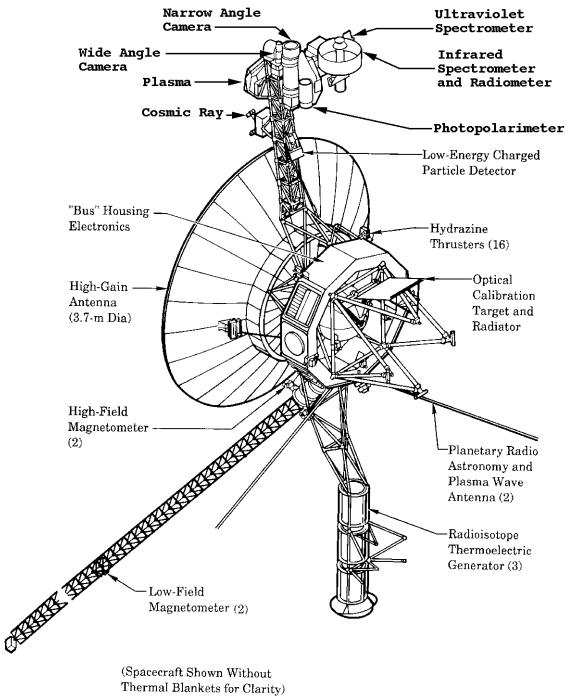

Figure 24: The Voyager Spacecraft

Investigator Teams	**Principal*** and Co-Investigators	
Plasma Science (PLS)	**J.D. Richardson***	R. McNutt
	J. W. Belcher	E.C. Sittler, Jr.
	L.F. Burlaga	C. Wang
	A.J. Lazarus	
Low-Energy Charged Particles (LECP)	**S.M. Krimigis***	L.J. Lanzerotti
	T.P. Armstrong	B.H. Mauk
	R.B. Decker	R. McNutt
	G. Gloeckler	E.C. Roelof
	D.C. Hamilton	
Cosmic Ray Subsystem (CRS)	**E.C. Stone***	F.B. McDonald
	A.C. Cummings	W.R. Webber
	N. Lal	
Magnetometer (MAG)	**N.F. Ness***	R.P. Lepping
	C. Smith	L.F. Burlaga
	F.M. Neubauer	J.P. Connerney
Plasma Wave	**D.A. Gurnett***	W.S. Kurth

Table 1: Voyager Investigations and Status

The Flight Data Subsystem (FDS) and an 8-track digital tape recorder (DTR) provide data handling functions. The FDS configures each instrument. controls instrument operations, collects engineering and science data and formats the data for transmission. The DTR is used to record high-rate PWS data, which are played back about four times per year on Voyager 1. The high rate PWS data on Voyager 2 are no longer useful, so Voyager 2 DTR operations have been terminated to conserve power.

The Computer Command Subsystem (CCS) provides sequencing and control functions. The CCS contains fixed routines, such as command decoding and fault detection, and corrective routines, antenna point-

ing information, and spacecraft sequencing information. The CCSs on both spacecraft are performing normally.

The Attitude and Articulation Control Subsystem (AACS) controls spacecraft orientation, maintains the pointing of the high gain antenna towards Earth, and controls attitude maneuvers. The Voyager 1 AACS circuitry was switched in 2002 and since then the redundant celestial sensors have been used. Following the switch, the new Canopus Star Tracker (CST) lost sensitivity at a higher rate than expected, but since December 2007 the rate of degradation has leveled off. The CST has no problem maintaining lock on the reference star or reacquiring the reference star after maneuvers. At the current rate of degradation, the star tracker should last until the end-of-mission.

Uplink communication is via S-band (16-bits/sec command rate) while an X-band transmitter provides downlink telemetry at 160 bits/sec normally and 1.4 kbps for playback of high-rate plasma wave data. Receiver 1 on Voyager 2 failed in 1978. Failure of the Tracking Loop Capacitor in Receiver 2 resulted in a drastic reduction in the acquisition frequency bandwidth, requiring the routine use of special procedures to determine the best lock frequency. Voyager 2 is currently operating on the alternate transmitter following an autonomous switch in 1998. The project has elected to remain on the currently selected transmitter. Telecommunications with both spacecraft are normal and the link margins are sufficient to maintain two-way contact with the spacecraft well after 2020.

Electrical power is supplied by three Radioisotope Thermoelectric Generators (RTGs) that are performing nominally. The current power levels are about 275 watts, with power margins of about 30 watts and an average degradation rate of about 4.3 watts per year. As the electrical power decreases, power loads on the spacecraft will have to be turned off, reducing spacecraft capabilities and operational flexibility. Power margins are adequate to operate the complement of science instruments, save the UVS, until after 2020. For power management, the UVS must be turned off in late 2010.

Spacecraft attitude is maintained by small hydrazine thrusters. One thruster has failed on Voyager 1 (Roll) and one on Voyager 2 (Pitch/Yaw). Additionally, the Pitch/Yaw thruster on Voyager 1 has shown signs of significant degradation, due to exceeding expected end-of-life usage. The thrusters currently in use are expected to last the rest of the mission. Nearly 1/3 of the original propellant remains available.

In late 2006, while performing an AACS test, uncommanded power relays were executed onboard Voyager 2. As a result, the magnetometer flippers were activated and the IRIS instrument was commanded on. Commands to return the spacecraft to the correct configuration were sent to the spacecraft and executed properly. A similar uncommanded execution of spacecraft systems occurred in 1998 when the scan platform on Voyager 2 was powered down. The flight team has isolated the probable circumstances that would cause this anomaly and have modified procedures and fault protection algorithms and has generated contingency plans to mitigate possible future occurrences.

In mid-2008 the CCS sent an unexpected power-on-reset command to the AACS, which caused the AACS to reinitialize. Though the reinitialization was normal, there was a loss of about 5 watts of power margin. Extensive investigation showed that all subsystems were operating normally, but did not reveal a cause for the loss of margin.

The PRA instruments on both spacecraft have been turned off to conserve power. As a result of the gain in power margin, gyro usage was extended to 2015 on Voyager 1 and to 2014 on Voyager 2 and Voyager 1 digital tape recorder usage was extended by 4 years to 2014,
.

9.3 Operations Concept

The VIM is characterized by (1) science requirements that can be satisfied with observations that are primarily repetitive in nature, and (2) long (and increasing) communication distances. The resulting long round-trip-light-times and decreasing signal levels significantly constrain spacecraft monitoring and control.

Programmatic changes since the beginning of the VIM have significantly reduced flight team staffing levels. As opposed to the multiple teams of specialists available earlier in the mission, each member of the current flight team performs multiple interdisciplinary functions and only limited backup capability exists.

These mission characteristics and the small team size have resulted in the evolution off the methods used to conduct mission operations. Multi-mission ground data systems are used, though Voyager requires some unique components to maintain compatibility with the multi-mission environment. Dramatic changes have been made to the process for real-time monitoring of routine spacecraft operations. Each of these is discussed further in the following sections.

The mission impact of the reduced staffing includes reduced operational flexibility, greatly reduced anomaly response capability, and potential delays in science data delivery. In addition, many important but non-critical tasks are not being performed.

9.4 Sequence Generation

The key to acquiring the desired science observations and maintaining an adequate level of mission adaptivity is the sequencing strategy. Because of the limited flight team resources available for spacecraft sequence generation, this strategy minimizes the labor

required while satisfying the science data acquisition requirements and flight system health and safety engineering needs.

Voyager's process of command sequence generation, review and uplink is unique to this mission. It requires continual support by Voyager-experienced personnel.

The sequencing strategy is composed of four basic elements. First is a continuously executing sequence of repetitive science observations and engineering calibrations called the "baseline sequence." A baseline sequence is stored on-board each spacecraft and contains the instructions needed to acquire and return the basic science data to the ground. This sequence will continue to execute for the duration of the mission, but requires periodic adjustment to deal with changes in spacecraft health and configuration, ground system capabilities and the heliospheric environment.

The second element is the storage on-board each spacecraft of the pointing information (HPOINTS) necessary to keep the boresight of the High Gain Antenna (HGA) pointed at the Earth. This provides the capability for continuous communication with each spacecraft without further HGA pointing commands. HGA Pointing Tables on both spacecraft were updated in 2009 to maintain the pointing accuracy needed for quality science data acquisition and to extend HPOINTS to the year 2029.

The third element provides the capability of augmenting the baseline sequence with non-repetitive science or engineering events using either an "overlay sequence," or a "mini-sequence." The difference between these two types of augmentation sequences is that the overlay sequence operates for a fixed interval of time, currently 3 months, and contains all of the baseline sequence augmentations for that time interval. A mini-sequence is focused on accomplishing a single augmentation need and is not a regularly scheduled activity but is done on an as-needed basis.

The fourth element is the use of pre-defined and validated blocks of commands (high level sequencing language), rather than the optimized sequence of individual commands (low level sequencing language) used during the prime mission, to accomplish desired spacecraft functions. The use of pre-defined blocks of commands greatly reduces the effort required to generate and validate a sequence of commands. The spacecraft contains pre-defined blocks of commands to support this functionality for routine activities.

9.5 Transmitting the Data to the Ground

The Voyager Interstellar Mission is, with one exception, a real-time data acquisition and return mission. All of the operating instruments on each spacecraft are continuously collecting data for immediate transmission to Earth. The normal real-time transmission data rate is 160 bits per second (bps), including 10 bps engineering data

The one exception to real time data return is that twice a week, 48 seconds of high rate (115.2 kbps) plasma wave data are recorded onto the DTR on Voyager 1. These data are played back about every 3 months and provide increased spectral resolution snapshots of the plasma wave information. Recording and playback of Voyager 1 high rate plasma wave data can continue until 2014, though antenna arraying will be necessary to capture the data.

9.6 Capturing the Data on the Ground

Real-time telemetry data capture is accomplished using 34- and 70-meter tracking antennas of the DSN. Capture of the recorded high rate plasma wave data from Voyager 1 requires the use of an array of 70- and 34-meter antennas.

Twelve hours per day of tracking support for each spacecraft is the project's target for science data acquisition. But because of oversubscription of the DSN, Voyager is usually allocated support after higher priority mission requirements have been satisfied. The recent daily support has averaged 8-10 hours. As tracking support is reduced, the ability to characterize the heliospheric medium is degraded. Acceptable minimum science data acquisition requirements range from 4 to 8 hours per day per spacecraft, depending on the specific investigation.

9.7 Delivery to Science Investigation Teams

Science data are provided electronically to the science investigation teams in the form of a Quick Look Experiment Data Record (QEDR) and Experiment Data Record (EDR). Voyager 1 and Voyager 2 QEDRs for each science investigation are generated daily (Monday through Friday) containing the available data since the last QEDR was produced. Since these products are produced in near real-time, generally within 24 hours of the data capture, data gaps due to a variety of ground system problems are present in the QEDR. Once a week, EDRs are created for the previous week's data which fill data gaps resulting from ground problems to the extent possible. When the final EDRs are available, science teams are notified by electronic mail. The science teams then retrieve the data at their convenience for further processing and analysis.

9.8 Spacecraft Monitor and Control

Spacecraft monitor and control includes the real-time functions necessary to monitor spacecraft health and to transmit and verify commands to insure data capture during special activities and support non-real-time functions. With the reduced flight team staffing during VIM and the acceptability of increased risk during an extended mission, real-time support is limited to weekday prime shift and special off-shift events (com-

manding, DTR playbacks, and attitude maneuvers). This reduced real-time monitoring support was enabled by the development and implementation by Voyager personnel of an automated telemetry monitoring tool which alerts on-call personnel to potential anomalous spacecraft conditions. This automation tool, Voyager Alarm Monitor Processor Including Remote Examination (VAMPIRE), has served as a model for development of a similar multi-mission tool now in use by other missions.

Maintaining spacecraft health and safety is a non-real-time function. It includes: the analysis of engineering telemetry data to establish and evaluate subsystem performance trends; the periodic in-flight execution and analysis of subsystem calibrations and engineering tests; analysis of AACS, FDS, and CCS memory readouts; the review and updating of telemetry alarm limits; the identification and analysis of anomalous conditions; and the implementation of corrective actions. Detailed anomaly analysis has suffered recently because of the level of staffing.

The analysis of engineering telemetry data to establish and evaluate subsystem performance trends is an important operations function. It drives decisions about future optimum configurations for maximizing mission lifetime. The analysis of these data relies on the system and subsystem expertise retained by the individual flight team members. Like anomaly analysis, as the flight team has lost subsystem expertise due to the retirement of experienced personnel and the downsizing of the flight team, the ability to perform trend analysis has been severely impacted. Though some new tools have been implemented over the last two years, which greatly assists in trend data display, development of an automated process for trend data analysis is considered a desirable future development to improve operations efficiency.

Periodic in-flight calibrations and engineering tests are used for verifying spacecraft performance, analyzing anomalies, and maintaining spacecraft capabilities. While some of these calibrations and tests are included in the baseline sequence, the majority are initiated from the ground in either an overlay or mini-sequence.

The identification and analysis of anomalous conditions and the determination of recommended corrective actions relies on the system and subsystem expertise of the individual flight team members. An automated tool, Monitor/Analyzer of Real-time Voyager Engineering Link (MARVEL) monitors CCS/FDS telemetry data to assist the analyst with normal event verification and to display on a workstation screen any conditions that are not as predicted. MARVEL performs limited analysis of the CCS/FDS telemetry and identifies possible causes of the anomalous condition and potential corrective actions from the stored knowledge base within the program.

9.9 Protection Against Spacecraft Failures

In order to maximize the spacecraft science data return reliability for a mission that could potentially continue until 2020 or beyond, automated safeguards against possible mission-catastrophic failures are provided.

Each spacecraft has Fault Protection Algorithms (FPAs) stored on-board that are designed to recover the spacecraft from otherwise mission-catastrophic failures. The FPAs are mostly implemented in the CCS although a few are interactive with the AACS. The five FPAs stored in the CCS execute pre-programmed recoveries for the following:

- AACS anomalies
- Loss of command reception capability
- Exciter and transmitter hardware anomalies
- CCS hardware and software anomalies
- Anomalous power loads

In addition, fault correction routines in the AACS deal with failures of its circuits and sensors.

The second safeguard is the Backup Mission Load (BML), which provides automated on-board protection against the permanent loss of command reception capability. Without command reception capability, the spacecraft must continue to operate with the instructions previously stored in the CCS memory. The BML reconfigures the spacecraft for maximum telecommunications and attitude control reliability and modifies the Baseline Load to continue the acquisition and transmission of fields, particles and waves science data as long as the spacecraft continues to function.

All of the above protection mechanisms require periodic review and occasional modifications by the Flight Team. These are dictated by planned configuration changes and by unpredictable changing conditions.

9.10 Consumables Management

Both spacecraft have on-board consumables that are adequate to support spacecraft operation until at least 2020. Electrical power is the major consumable which limits the spacecraft lifetime. Power should be adequate to support science data acquisition until at least 2020 and possibly beyond. Both spacecraft have about 30 kg of hydrazine that provides about 50 years of operation at current usage rates.

9.11 Mission Adaptivity

While Voyager is primarily a non-adaptive real-time data acquisition and return mission, two types of science data acquisition and return adaptivity exist. Both types have been successfully used during VIM.

The first type of adaptivity is the recovery of a high rate PWS playback that is not captured with the initial playback. The response to the loss of a playback is to sequence a second playback prior to the time

when data on the DTR is overwritten with newly recorded data. For normal baseline sequence recording of PWS data this allows 6 months to execute a second playback.

The second type of adaptivity is to increase the frequency of high rate PWS recordings and playbacks. This was done in response to increased plasma wave activity during cruise and the predicted Voyager 1 termination shock crossing and has continued so as to monitor plasma wave activity within the heliosheath and originating from the heliopause. An on-board sequence block allows increasing the high rate PWS recordings by sending a single command to the spacecraft. It can record one PWS frame about every nine hours over a period of two weeks or one additional frame per week for six months. The latter mode is in use on Voyager 1 and doubles the resolution of the PWS high-rate data.

9.12 Science Management

The Project Scientist coordinates with the Voyager Science Investigators, the science community, and other elements of the Project to ensure that the Project scientific objectives are met. The Science Steering Group (SSG) is chaired by the Project Scientist and consists of the Principal Investigators for the funded investigations (see Table 2). The SSG has the leading role in the overall optimization of the science return from the mission and in the resolution of conflicting science requirements.

Although funding for UVS has been discontinued by NASA, the data set is still being received and then made available to Jay Holberg at the University of Arizona. As mentioned earlier, the PRA instruments on both spacecraft have been turned off for power conservation.

The principal investigators are responsible for analyzing their data and reporting their findings in a timely manner. They participate, as appropriate, in making these results available to the science community and to the general public. They present their results at science conferences, through news releases and via publications in the popular press and scientific journals. A list of published papers, by investigation, is available at http://voyager.jpl.nasa.gov/science/bibliography.html

The principal investigators provide archival data to the National Space Science Data Center at Goddard. Archived data can be accessed via the NSSDC Master Catalog at the following URL: http://nssdc.gsfc.nasa.gov/planetary/voyager.html

A summary of data availability is accessible at the Virtual Space Physics Observatory at http://vspo.gsfc.nasa.gov/websearch/dispatcher

In addition, a list of URL's, which point to science data, including those at the investigators' home institutions, is located at the JPL Voyager web site at http://voyager.jpl.nasa.gov/ .

11 VOYAGER EPO PROPOSAL

11.1 Overview

The Voyagers, the most distant human-made spacecraft, are currently exploring the heliosheath. As part of the Heliophysics System Observatory (HSO), the Voyager spacecraft provide a unique set of heliophysics data that support the HSO goals. During the mission's life-cycle, the education and public outreach (EPO) efforts of the project will continue to be focused primarily on the improvement and productivity of Science Technology, Engineering & Mathematics (STEM) learning for grades K-14 to ensure a coordinated, balanced and broad portfolio of activities in formal, informal and public outreach. Through collaborations and partnerships we will engage students and sustain their interest in heliophysics-related subjects.

11.2 Education And Public Outreach Plan Fy10-Fy14

11.2.1 Formal Education

The Voyager Education and Public Outreach Coordinator will continue to attend the National Science Teachers Convention. The mission EPO Lead is an invited participant in the live webcast from NSTA 2010 in Philadelphia. We will continue to support the California Science Teachers Meeting by submitting workshop proposals and supporting the NASA exhibit.

In October 2009 in collaboration with Stereo, Genesis, Ulysses, and the JPL Education Office, Voyager hosted the first Sun Educator Workshop at JPL. The workshop combined four heliospheric mission presentations with one Earth Science presentation followed by a NASA approved activity related to the mission or presentation. Activities are led by an Education Specialist or Educator. We have committed to having one workshop a year using the 2009 model.

Figure 25: Teachers teaming up on sun activity during workshop

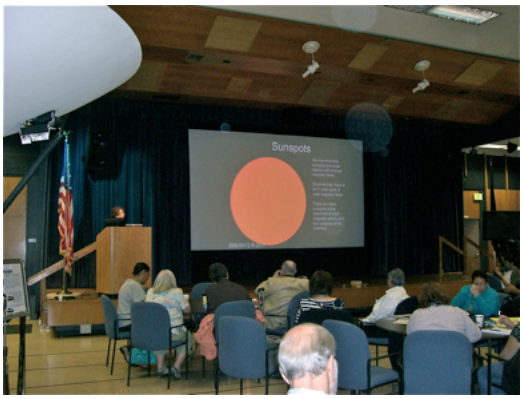

Figure 26: Dr Paulett Liewer presents sun data from STEREO mission

The Voyager team members at the University of Iowa will continue to support the Local Boy Scout troops. This effort assists troop members in attaining the Space Exploration Merit Badge. The University of Iowa held a Merit Badge University Class in March 2009. Eighteen Scouts received merit badges by participating in discussion and activities related to the Voyager, Cassini, Mars Express and Juno missions.

11.2.2 Informal Education

Voyager will continue its 9-year partnership with the NASA/JPL Ambassador Program. Project team members will keep ambassadors informed of Voyager status and discoveries in the heliosheath via teleconference updates

with key Voyager science team members and spacecraft engineers.

As a partner in the redevelopment of the Space Weather Media Viewer, Voyager will support education of the 3D Heliosphere and the Solar Cycle. (http://sunearth.gsfc.nasa.gov/spaceweather/FlexApp/bin-debug/index.html#). By producing and supplying new, innovative illustrations and explanations of the inner and outer heliosphere and scientist interviews (ACE, HINODE, IBEX, SOHO, STEREO, THEMIS and Voyager missions), we will tell a more complete story of the Heliosphere. The Viewer is a national resource for educators and the general public. The Annual EPO Sun-Earth Day 2009 reported direct training of 3146 educators, students and parents using the viewer. During just one week in December 2009 the Viewer had 126,118 hits and 7181 unique geographically diverse domestic and international visitors.

The Voyager project will continue as the JPL lead for the National Sun-Earth Day activities (http://sunearthday.nasa.gov/2010/getinvolved/ideas.php). In March 2009, the project hosted ~100 elementary school students for the NASA led Webcast. There were four students from the JPL group that participated in the webcast by interacting and asking questions of NASA Scientist, Engineers and Education Specialist.

Figure 27: Student asks questions during SED webcast

The students then participated in a presentation from the STEREO team and had the opportunity to view blue ray disk images of the Sun. Associated activities were then demonstrated on the JPL Mall while the students used solar telescopes to view the Sun safely.

Figure 28: Sun-Earth Day at JPL

The Voyager Project commits to two K-12 class tours of JPL each year. The first-hand experience of a NASA Research and Development laboratory builds awareness among students, educators, and the public on the diverse range of career opportunities related to heliophysics science and missions.

In collaboration with The Space Place, the Voyager Project EPO Lead will work to develop an explanation of the Heliosphere and the Sun-Earth-System for elementary school students. A Voyager Space Place Fun Fact activity using the "Kitchen Sink" animation will be developed in English and Spanish. There will also be an Astro Space article at the time the activity goes live. The idea is to start early with the correct information and images to create a lasting impression while having fun. (http://spaceplace.nasa.gov/en/kids/faq.shtml)

11.2.3 Public Outreach

The Voyager Project will continue to participate in the annual JPL Open

House event. The event provides the Voyager mission a venue to discuss and share heliophysics science and outreach materials with over 30,000 members of the general public each year.

Figure 29: Voyager team volunteers at JPL Open House

The project Scientist and Engineers will continue to speak to various public organizations and civic groups such as the Aerospace and Electronics Systems, Life Members, and local Rotary Clubs. We work closely with the JPL Speakers Bureau on special requests for these organizations and K-14 schools.

11.2.4 Products

The Voyager educational wall sheet is regularly requested for Sun-Earth-Day packets and NASA represented conferences and is downloaded monthly in large quantities from the Voyager web site. We will reproduce the wall sheet with updated images that reflect the Voyagers current locations and mission profiles. We will work with the JPL Education office to have the poster translated to Spanish. We will produce a new exhibit background for the JPL Open House event.

11.2.5 Evaluation

Each product will go through formative evaluation. Teacher-advisors will evaluate each product for age appropriateness, choice of medium and support materials. Selected museum partners also have an opportunity to review the concept. The summative evaluation component is conducted by the Program Evaluation & Research Group (PERG). Using pre- and post-testing and informal interviews we will assess educational merit. The NASA SMD Education Product Review process is completed before development of any product. The Voyager Project will use the NASA Office of Education Performance Measurement (OEPM) Student End of Event Surveys.

11.3 E/PO Budget

As part of NASA's Science Mission Directorate (SMD), the Voyager project will continue to leverage its limited E/PO funds through partnerships/subcontracts such as the Solar System Ambassadors (SSA) Program. We will supply materials such as educational posters, bookmarks, and power point presentations for these events to aid committed volunteers in representing NASA missions. The requested funds include future updates to the Space Weather Viewer, design and development of the Space Place "Fun Fact", Astro Club space article and JPL Virtual Field Trip. Requested consultant fund will cover language translation for Voyager products. Travel funds are requested to attend the NASA supported conferences, education workshops and science conferences where Voyager is represented. Direct labor costs will cover Voyager web site updates, audiovisual support, and graphic services.

	FY-09	FY-10	FY-11	FY-12
1. Direct Labor (salaries, wages, and fringe benefits)	8000	8000	8000	8000
2. Other Direct Costs:				
a. Subcontracts	33000	33000	33000	33000
b. Consultants	2000	2000	2000	2000
c. Equipment				
d. Supplies	3000	3000	3000	3000
e. Travel	4000	4000	4000	4000
f. Other				
3. Facilities and Administrative Costs				
4. Other Applicable Costs				
5. SUBTOTAL--Estimated Costs	50000	50000	50000	50000
6. Less Proposed Cost Sharing (if any)				
7. **Total E/PO Estimated Costs**	50000	50000	50000	50000

Table 2: EPO Budget

12 Mission Archiving Plan

12.1 INTRODUCTION

The Voyager Interstellar Mission is, with one exception, a real-time data acquisition and return mission. All of the operating instruments on each spacecraft are continuously collecting data for immediate transmission to Earth. The normal real-time transmission data rate is 160 bits per second (bps), including 10 bps engineering data

The one exception to real time data return is that twice a week, 48 seconds of high rate (115.2 kbps) plasma wave data are recorded onto the DTR on Voyager 1. These data are played back about every 3 months and provide increased spectral resolution snapshots of the plasma wave information. These high rate plasma wave data provide the primary data for the Plasma Wave Investigation Team's estimate of the termination shock and heliopause locations. Recording and playback of Voyager 1 high rate plasma wave data can continue until 2014 when the digital tape recorder must be turned off for power management.

12.2 DATA ANALYSIS AND ARCHIVING

The principal investigators are responsible for analyzing their data and reporting their findings in a timely manner. They participate, as appropriate, in making these results available to the science community and to the general public.

The principal investigators provide archival data to the National Space Science Data Center at Goddard. Archived data can be accessed via the NSSDC Voyager Project Information Page at the following URL:

http://nssdc.gsfc.nasa.gov/planetary/voyager.html

A listing of data availability, including access links, is available at the Virtual Space Physics Observatory at http://vspo.gsfc.nasa.gov/websearch/dispatcher. In addition, a list of URL's, which point to science data, including those at the investigators' home institutions, is located at the JPL Voyager web site at http://voyager.jpl.nasa.gov/.

Data collected during the planetary encounters are archived at the Planetary Data System (PDS) at http://pds.jpl.nasa.gov/. All data from the Plasma Wave Spectrometer instrument are already being archived at the PDS. In the very near future, data from the Low-energy Charged Particles and the Plasma Science instruments during their time in the solar wind will be available online at the PDS.

12.3 LOW ENERGY CHARGED PARTICLES (LECP)

Low Energy Charged Particle observations are archived at three sites

1. Fundamental Technologies, LLC http://data.ftecs.com/archive/voyager_lecp/index.html
2. The Johns Hopkins University Applied Physics Laboratory http://sd-www.jhuapl.edu/VOYAGER/index.html
3. The University of Maryland http://voyager-mac.umd.edu/

Additionally, the Planetary Data System (PDS) at UCLA has arranged with Tom Armstrong for an LECP data node to get LECP energetic particle data into the PDS. Dr. Armstrong has completed the coding of a VAX procedure that will create listings in CSV form of the LECP Cruise 5A rate data at maximum time resolution. The delivery, with label files, to the PDS will include all the rate channels in a single print file in time order. Delivery is expected to begin soon.

The organization of the data is approximately as follows:

Fundamental Technologies, LLC has compiled all of the counting rate channel observations from launch to the latest available at cadences ranging from the highest time resolution, which varies widely with mission phase, through step-synchronous, scan-synchronous, hourly, and daily cadences. For the planetary encounters the ancillary observations of trajectory and magnetic field derived parameters are included at a cadence that lets them be joined in spreadsheets to form customized data sets for any suitable purpose. All of the observations are rendered in two forms, comma separated (CSV) ASCII (flat) files and binary (provided for inputs to special purposes LECP software). The CSV files will open as column labeled spreadsheets with one complete record per spreadsheet line. Calibration of count rates into fluxes is accomplished by dividing by (geometrical factor) × (delta-energy) products that are located in the files to be found in http://data.ftecs.com/archive/voyager_lecp/Explanations/STEP-files.html for example.

Extensive documentation of the technical aspects of the LECP instrument derived from engineering design memos, laboratory calibration, and computer modeling are also to be found in the ftecs web site at http://voyager.ftecs.com/.

Johns Hopkins University Applied Physics Laboratory posts the latest polished results from the LECP investigation along with important metadata and related works, especially journal publications. Posted data include browse plots of latest data and flat files of angular and scan-averaged intensities of key channels from launch onward.

The University of Maryland (UMD) offers the

results of the LECP investigation derived from the pulse height analysis mode of the Low Energy Particle Telescope (LEPT). The UMD website presents 26-day, 52-day, and annual flux averages for several species as a function of energy. Plots are updated automatically approximately weekly. All data returned in the Cruise 5a format are included. The covered time period is Day 228, 1990 to the present. No planetary flybys are included. Two types of plots are available: time-intensity plots and spectra plots. Time-intensity plots are provided for H, He, C, and O for three energy ranges near 1 MeV, 6 MeV, and 25 MeV. Energy spectra are provided for those and additional species over the entire LEPT energy range.

12.4 COSMIC RAY SUBSYSTEM (CRS)

The CRS team preserves all instrument data received as Experiment Data Records (EDRs) in the EDR library. The primary data repository used for instrument validation and science analysis is the Encyclopedia, generated from EDRs, which consists of 15 minute volumes. A volume consists of one or more chapters. Each chapter contains CRS science data, acquired in a single instrument mode, and the associated CRS engineering measurements and relevant spacecraft engineering data. A chapter consists of one or more verses. Verses of a chapter contain measurements of one of the several types of measurements (counting rates, pulse heights satisfying specific coincidence requirements), made during the time period covered by the chapter. The classification of pulse height data into verses is based on tag information generated onboard. With the exception of data where the status information contained in the EDR is not sufficient to identify the instrument state, the encyclopedia contains all the data, tagged with available quality information. Subsets of the encyclopedia containing selected verses for a specified time period can be created from the master encyclopedia.

Generally speaking, CRS data products are generated on demand, at user specified temporal averaging (multiple of 15 minutes), and consist of counting rates and fluxes for the species and energy ranges required by the science investigation. While it is possible to extract data at the instrument resolution, these data have rarely been used except during planetary encounters. EDR and Encyclopedia formats are well documented. Programs used to create these products are written in C.

CRS team makes available 6-hour, daily and 26-day data listings and yearly plots for 14 Hydrogen and Helium intensities and two counting rates at the CRS website http://voyager.gsfc.nasa.gov.

Six hour and daily averages of all CRS counting rates (excluding planetary encounter periods) are available at the NSSDC at ftp://nssdcftp.gsfc.nasa.gov/spacecraft_data/voyager/voyager1/particle/crs/ and ftp://nssdcftp.gsfc.nasa.gov/spacecraft_data/voyager/voyager2/particle/crs/. Additional products (15 minute averages and daily averages of intensities) are accessible via the Virtual Energetic Particle Observatory (VEPO) website http://vepo.gsfc.nasa.gov. Capabilities to browse all count rates and pulse height data interactively have been developed, and will be made accessible as web services.

The CRS website provides a description of the detector systems, and references to more detailed description in the literature. The website also lists time periods where data quality is suspect and documents the nature and instances of anomalous detector system response.

Since CRS products are created on demand from the encyclopedia which is updated when an EDR is received, no significant action is necessary for completing production of data products that are generated at present. However, for effective long-term use of CRS data, we will need to do the following:

1. In cooperation with the VEPO and SPASE, develop an interface for delivering flux, associated statistical uncertainty and components involved in the computation.
2. In consultation with VEPO and SPASE, create an encyclopedia reader API that extracts rates and pulse height data from an encyclopedia in a compliant form.
3. Create middleware that allows web services to interface with the encyclopedia via the encyclopedia reader API.

We expect that bulk of the work outlined above can be accomplished as part of our contribution to the VEPO effort, and we will be well placed to move to resident archive phase.

Documentation on the CRS website will include:

1. Reformatted instrument description, including drawings showing geometry.
2. Detailed documentation of detector system characteristics, and response tables and algorithms used to identify particle species and to determine particle energy. In addition to allowing validation of CRS results by potential users, this will allow a user to determine the overlap, if any, between the (particle species, energy range) of interest and the parts of the (particle species, energy range) space measured by CRS. In case the quantity of interest is measured by more than one of CRS detector systems, this document will provide additional information to allow the user to select a source appropriate to the query.

3. Updated list of time periods where data quality is suspect
4. Updated documentation of nature and instances of anomalous detector system response.
5. Data Availability documentation will provide a closer look than that provided by the telemetry coverage of the spacecraft, and will help the user determine times when CRS was in a configuration appropriate to making the desired measurement.

Data products delivered by CRS consist of counting rates, and fluxes for the species and energy ranges requested by the user. CRS web services will deliver these in containers conforming to the SPASE compliant framework expected to be developed by the VEPO. These containers and services that provide the content will be registered with relevant virtual observatories, such as the VEPO.
The following analysis tools will be provided to the community:

1. Web based clients to request time histories and spectra from CRS web services
2. Web based browser for CRS pulse heights.
3. As part of our work on VEPO, we expect to develop tools for correlating CRS measurements with other energetic particles and magnetic field measurements.

All data will be made available via web services. Users will be able to request fluxes and/or counting rates of interest. In the long term, these will be delivered in containers conforming to SPASE based community standards developed by the VEPO. If an encyclopedia, containing all, or a subset of data types is requested, users will be able to carry out their own analysis using the above mentioned Encyclopedia reader API registered with the VEPO. As mentioned above, programs that read encyclopedia will need to be adapted to make use of Encyclopedia reader API.

12.5 MAGNETOMETER

12.5.1 Introduction

The Heliophysics Data Management Policy assumes that the processing of data from missions in their extended phase is routine. This is NOT the case for the Voyager magnetometers. New methods had to be developed and major revisions of the processing system were developed to measure the very weak magnetic fields in the distant heliosphere in the presence of the relatively large and variable magnetic fields generated by the spacecraft. Most recently, the processing methods and data processing system had to be modified very significantly to deal with the damage to the V2 outboard sensor triad discussed below, and these methods might have to be changed further as we learn more about the behavior of that sensor. Further modifications in both the V1 and V2 data processing will have to be made as the spacecraft move farther into the heliosheath.

Present Archive

Hour averages and 24-hour averages of the magnetic field strength F1, F2 and the IHG components BR, BT, BN are deposited in the NSSDC at ftp://nssdcftp.gsfc.nasa.gov/spacecraft_data/voyager/voyager1/magnetic_fields/ and ftp://nssdcftp.gsfc.nasa.gov/spacecraft_data/voyager/voyager2/magnetic_fields/ and are also made available to the community on COHOWeb at http://cohoweb.gsfc.nasa.gov/. These magnetic field data are available for the entire mission, up to current processing and validation. The documentation, which includes essential information on the uncertainties of the measurements, accompanies the data on COHOWeb. All planetary encounter data from Voyager 1 and Voyager 2 are available at COHOWeb and at the PDS at http://pds-ppi.igpp.ucla.edu/data.htm

12.5.2 Data

All of the measurements of the magnetic field are on the EDRs (Experiment Data Records). These are stored on a disk and on CDs at GSFC, and they are also available from JPL. Other data needed for processing (attitude, etc) are in the SEDRs, which are available online. Extraction of these data requires both standard routines, that are stored at GSFC, and special adaptations that are required to deal with special problems that arise in the acquisition and transmission of the data. Processing of the data requires extensive tabulations of "zero tables" and the processing program itself, which are available at GSFC. The processing program is documented partially online at the MAG web site. The process of constructing zero tables and the processing program are still evolving, owing to changes in the heliospheric environment, the instruments, and the S/C generated magnetic field behavior.

12.5.3 Instrument Status

The Voyager 1 magnetometer (inboard and outboard sensors and electronics) continues to operate nominally, although the spacecraft magnetic field remains comparable to or greater than the magnetic fields being measured, even in the heliosheath. The Voyager 2 outboard magnetometer was damaged in 2006 as a result of a command to the spacecraft, which had the unintended consequence of activating the heater and flipper of the outboard sensor triad, and the elapse of a week before the heater was turned off. The resulting high temperatures (too high to be measured) exceeded the design limits. This had two serious consequences. 1) The outboard sensor was rotated to a position between the two nominal operating positions.

2) There appears to be damage to wires and/or other electronic components, resulting in large and variable changes in the zero levels. The orientation of the sensor was determined by use of the calibration coil on the S/C. However, there is no reason to assume that this new orientation will remain fixed. It will be necessary to monitor the orientation, which requires periodic S/C commands to exercise the calibration coil, with attendant risks.

12.5.4 Data Processing

The current data reduction method requires the determination of the zero level of each component of each of the two sensors every 48 seconds. The zero tables are constructed manually. This is a very labor intensive procedure. Given the decreasing budget, we will try to find ways to automate this process to some degree. In any case, there is no standard procedure that could be implemented by members of the outside community.

A further problem in data processing is unresolved but crucial in the heliosheath. The spacecraft rolls, which are essential for calibration, are essentially about the "R" axis pointing toward earth (and sun). We have determined the zero-offset in the R component by assuming that the average of the R component for 52 days, centered at the time of a roll, is zero. This is reasonable in the supersonic solar wind, where BR decreases as $1/R^2$, where R is the distance from the sun. (At 100 AU, the magnitude of BR is of the order of 6/(100x100) = 0.0006 nT, well below the digitization limit). In the heliosheath, one expects the magnetic field to eventually be deflected away from the spiral direction so that it becomes nearly parallel to the heliopause. This implies that a significant component of BR will exist in the heliosheath, so that the assumption
 = 0 is no longer valid. This problem is complicated by the fact that the outboard sensor triad on V2 has been rotated such that there is no longer only one sensor axis sensitive to the magnetic field component in the R direction.

12.5.5 High-Resolution Observations

In principle, the processing system produces averages of the basic sample period (0.48 sec) of the magnetic field at 1.92 sec, 9.6 sec, and 48 sec intervals. Previously, all of these data were stored on a mass storage system at GSFC, but cost, efficiency and practical considerations forced us to abandon this procedure. We no longer have a digital archive of the high resolution observations, and we no longer routinely produce the high-resolution data. Currently, we produce high-resolution data for limited intervals by reprocessing the data for those intervals, in a manner optimized for specific scientific studies.

12.5.6 Software

The program(s) to process the data are stored at GSFC. Partial documentation of the program is available on the Internet through the MAG site. However, at this stage, the processing is not routine and requires special expertise by experienced and well trained personnel.

12.6 PLASMA SCIENCE (PLS)

The MIT PLS data is archived at MIT on http://web.mit.edu/space/www/voyager.html which has fine-resolution, hourly and daily average data from launch. This web site also has a description of the data and a list of publications using the data.

COHOweb (http://cohoweb.gsfc.nasa.gov/) also has the PLS data which is picks up periodically from the MIT web page. They have meta-data on the instrument and graphical and analysis interfaces.

The NSSDC also picks up the PLS data and stores it at ftp://nssdcftp.gsfc.nasa.gov/spacecraft_data/voyager/voyager2/plasma/. The NSSDC has a very complete description of the instrument and data products.

The Voyager 1 and 2 PLS interplanetary data have also been copied to the Planetary Data System at UCLA but are not yet on-line.

12.7 PLASMA WAVE SUBSYSTEM

The Voyager PWS data has been archived with the Planetary Data System (PDS) Planetary Interactions (PPI) Node (http://pds-ppi.igpp.ucla.edu/) beginning with the planetary flyby data (Jupiter, Saturn, Uranus, and Neptune) and more recently 'entire mission' archives have been submitted including the cruise data before, between, and after the planetary flybys. While all the data are relevant to various aspects of Heliophysics, the latter are most relevant to the current Voyager Interstellar Mission. PWS data are archived in two primary data sets. The first of these are the spectrum analyzer data from the 16-channel receivers on each spacecraft covering the frequency range from 10 Hz to 56 kHz and which are acquired continuously (while the spacecraft are being tracked by the DSN). The second comprise wideband waveform data which cover the frequency range from 50 Hz to 12 kHz and which are recorded infrequently and played back on a quasi-periodic basis from the spacecraft tape recorder. All PDS data are provided to the National Space Science Data Center (NSSDC) as the deep archive.

Summary of Voyager PWS data sets submitted to PDS:

1. Voyager 1 PWS full resolution uncalibrated spectrum analyzer data
2. Voyager 2 PWS full resolution uncalibrated spectrum analyzer data

3. Voyager 1 PWS hourly average calibrated spectrum analyzer data
4. Voyager 2 PWS hourly average calibrated spectrum analyzer data
5. Voyager 1 PWS full resolution uncalibrated waveform data (Note that PWS does not return automatic gain control information for the waveform receiver, hence, waveform data cannot be absolutely calibrated.)
6. Voyager 2 PWS full resolution uncalibrated waveform data through August 2003. (Note that the Voyager 2 waveform receiver started to degrade in May, 2001 and was declared failed by August 2003, after which data were no longer usable. The same note about lack of gain information for the Voyager 1 instrument applies to Voyager 2, hence, no absolute calibration is possible for this data set.)

To be accepted by the PDS, data sets are required to have sufficient documentation such that a user can read and analyze the data. Hence, each of the PWS PDS data sets has catalog files which describe the mission, the spacecraft, and the instrument and also describe the data sets, and how they were derived. Also included is the Space Science Reviews paper by Scarf and Gurnett (1977) describing the investigation, its objectives, and the instrumentation. Detailed information including algorithms on reading the data and applying calibration transformations are included along with input/output file pairs so that a user can verify that any new software is returning the correct values. The PDS data sets also have label files for each of the data files that provide information required to locate data of interest (primarily by target and date/time). Browse files are also available which enable a user to view the data with only a web browser. Links from the browse data to both the data and metadata are provided as well as analysis software.

In addition to the PDS data sets, which are updated on a time scale of once per year or so, all of the PWS PDS-archived data plus any more recent data are available on a web site at the University of Iowa (http://www-pw.physics.uiowa.edu/voyager/). The web site includes access to all documentation included with the PDS data sets as well as software which will provide the data in the form of either plots or calibrated listings in electronic form. Information needed to work with the data is also included here, including code fragments and algorithms. Pointing information is not usually needed for the analysis of PWS data because of the broad field of view afforded by the dipole antenna. Ephemeris data in the form of SPICE kernels are available from either the Navigation and Ancillary Information Facility (NAIF) at the Jet Propulsion Laboratory (http://naif.jpl.nasa.gov/naif/) or the PDS. Plots or listings of the Voyager positions are also available via tools at the NSSDC (http://nssdc.gsfc.nasa.gov/space/helios/heli.html). Also, plotting tools available at the University of Iowa web site list the spacecraft position as a function of time.

While full resolution calibrated spectrum analyzer listings are available from the University of Iowa web site, it is our plan to add to the PDS data sets a fully calibrated, full resolution data set for each of the instruments in an ASCII flat file format.

Voyager PWS data will be consistent with the NASA Heliophysics Science Data Management Policy and will be available through the Virtual Observatories. SPASE (Space Physics Archive Search and Extract) metadata will be generated for the Voyager data and they will be available through the VxO (Virtual Observatory) system. The personnel at the PDS PPI node also sponsor a Virtual Magnetospheric Observatory (VMO), hence, are well aware of the SPASE data model and are developing tools to convert PDS metadata into SPASE compatible metatadata. Hence, the data archived with the PDS PPI node will have a direct link to the VMO. The current VHO (Virtual Heliospheric Observatory) does not serve any heliospheric wave data but the VMO and VHO plan to share facilities at Goddard Spaceflight Center, hence, the VMO (which will hold wave data) will be available to the VHO, as well.

SUMMARY OF LINKS TO VOYAGER DATA

Experiment	Links
All Experiments	Virtual Space Physics Observatory: http://vspo.gsfc.nasa.gov/websearch/dispatcher COHOweb: http://cohoweb.gsfc.nasa.gov/ NSSDC: http://nssdcftp.gsfc.nasa.gov/spacecraft_data/voyager/
CRS	GSFC: http://voyager.gsfc.nasa.gov.
LECP	Fundamental Technologies: http://data.ftecs.com/archive/voyager_lecp/index.html Applied Physics Lab: http://sd-www.jhuapl.edu/VOYAGER/index.html Univ of MD: http://voyager-mac.umd.edu/
MAG	ftp://nssdcftp.gsfc.nasa.gov/spacecraft_data/voyager/voyager1/magnetic_fields/ ftp://nssdcftp.gsfc.nasa.gov/spacecraft_data/voyager/voyager2/magnetic_fields/
PLS	MIT: http://web.mit.edu/space/www/voyager.html
PWS	Univ of Iowa: http://www-pw.physics.uiowa.edu/voyager/ Planetary Data System, PPI Node: http://pds-ppi.igpp.ucla.edu/

Appendix 1
List of Acronyms

Acronym	Meaning
$xsxK	Thousands Of Dollars
AACS	Attitude & Articulation Control Subsystem
ACE	Advanced Composition Explorer
ACR	Anomalous Cosmic Ray
AMMOS	Advanced Multi-Mission Operations System
API	Application Programming Interface
AU	Astronomical Unit
B	Magnetic Flux
BEST	Better Educated Students for Tomorrow
BML	Backup Mission Load
BS	Bow Shock
C	Carbon
CCS	Computer Command Subsystem
CIR	Corotating Interaction Region
CMIR	Corotating Merged Interaction Region
CR	Carrington Rotation
CRS	Cosmic Ray Subsystem Experiment
CSV	Comma Separated Values
DOY	Day of Year
DSA	Diffusive Shock Acceleration
DSN	Deep Space Network
DTR	Digital Tape Recorder
E/PO, EPO	Education & Public Outreach
EDR	Experiment Data Record
ENA	Energetic Neutral Atom
eV	electron volt
FDS	Flight Data Subsystem
Fe	Iron
FPA	Fault Protection Algorithm
FTE	Full-Time Equivalent
GAL	Galactic Plane
GCR	Galactic Cosmic Ray
GMIR	Global Merged Interaction Region
GONG	Global Oscillation Network Group
GSFC	Goddard Space Flight Center
H	hydrogen
HCS	Heliospheric Current Sheet
HDP	Hydrogen Deflection Plane
He	Helium
HGA	High-Gain Antenna
HP	Heliopause
HSH	Heliosheath
HSO	Heliophysics System Observatory
IBEX	Interstellar Boundary Explorer
ICME	Interplanetary Coronal Mass Ejection
IMF	Interplanetary Medium
IMP	Interplanetary Monitoring Platform
IRIS	Infrared Interferometer Spectrometer and Radiometer
ISM	Interstellar Medium
ISMF	Interstellar Magnetic Field
JPL	Jet Propulsion Laboratory
K	kelvin (degrees)
K-12	Kindergarten through 12th grade
K-14	Kindergarten through Undergraduate
keV	Thousands of Electron Volts
kHz	kilohertz
LECP	Low-Energy Charged Particles
LISM	Local Interstellar Medium
Lyman α	Lyman Alpha
MAG	Magnetometer Experiment
MARVEL	Monitor/Analyzer Of Real-Time Voyager Engineering Link
MeV	Million Electron Volts
MFP	Mean free path
MHD	Magnetohydrodynamics
μG	microgauss
MIR	Merged Interaction Region
MIT	Massachusetts Institute of Technology
NASA	National Aeronautics & Space Administration
Ne	neon
NSSDC	National Space Science Data Center
NSTA	National Science Teachers Association
nuc	Nucleon
O	oxygen
PDS	Planetary Data System
PERG	Program Evaluation & Research Group
PLS	Plasma Science Experiment
PRA	Planetary Radio Astronomy
PUI	Pickup Ions
PWS	Plasma Wave Subsystem Experiment
QEDR	Quicklook EDR
RTG	Radioisotope Thermoelectric Generator
SMD	Science Missions Directorate
SOHO	Solar & Heliospheric Observatory
SPASE	Space Physics Archive Search & Extract
SSA	Solar System Ambassadors
SSG	Science Steering Group
SSSC	Sun-Solar System Connection
STEM	Science Technology, Engineering & Mathematics
SW	Solar Wind
TS	Termination Shock
TSP	Termination Shock Particles

Acronym	Meaning
URL	Uniform Resource Locater
UT	Universal Time
UVS	Ultra-Violet Spectrometer
V	Velocity
V1	Voyager 1
V2	Voyager 2
VAMPIRE	Voyager Alarm Monitor Processor Including Remote Examination
VEPO	Virtual Energetic Particles Observatory
VHO	Virtual Heliophysics Observatory
VIM	Voyager Interstellar Mission
VMO	Virtual Magnetospheric Observatory